Natural Resources Canada | Ressources naturelles Canada

GEOLOGICAL SURVEY OF CANADA
OPEN FILE 8898

Assessment of physicochemical properties in lentic water bodies of the Rankin Inlet area (Nunavut) for sublacustrine open talik detection

B. Faucher, A.-M. LeBlanc, N. Utting, and M. Blade

2022

Canada

GEOLOGICAL SURVEY OF CANADA
OPEN FILE 8898

Assessment of physicochemical properties in lentic water bodies of the Rankin Inlet area (Nunavut) for sublacustrine open talik detection

B. Faucher[1], A.-M. LeBlanc[1], N. Utting[2], and M. Blade[3]

[1]Geological Survey of Canada, 601 Booth Street, Ottawa, Ontario
[2] Natural Resources Canada, CanmetENERGY, 1 Oil Patch Drive, Devon, Alberta
[3]Government of Nunavut, Department of Community and Government Services (CGS), P.O. Box 1000, Station 7, 4th Floor, Iqaluit, Nunavut

2022

Permanent link: https://doi.org/10.4095/330212

This publication is available for free download through GEOSCAN (https://geoscan.nrcan.gc.ca/).

Recommended citation
Faucher, B., LeBlanc, A.-M., Utting, N., and Blade, M., 2022. Assessment of physicochemical properties in lentic water bodies of the Rankin Inlet area (Nunavut) for sublacustrine open talik detection; Geological Survey of Canada, Open File 8898, 33 p. https://doi.org/10.4095/330212

Publications in this series have not been edited; they are released as submitted by the author.

SUMMARY

In periglacial landscapes of Northern Canada, the presence of open taliks (layer of unfrozen ground that penetrates permafrost completely) beneath lakes can connect surface waters to subpermafrost groundwater. With increasing mining activity in northern Canada, it is critical for mining projects to identify lakes potentially underlain by open taliks and their subpermafrost groundwater-surface water connectivity to assess effects on mining operations and lake water levels, lake water quality, and regional groundwater systems. The presence of sublacustrine open taliks can be assessed with thermal models, but validating their presence remains challenging at a regional scale due to the difficulty and cost of acquiring field data at this scale. The level of hydrological connectivity between the lakes and subpermafrost groundwater systems also remains largely unknown. This work explores the physical attributes and water chemistry of lakes in the Rankin Inlet area (NU) to infer the presence of open talik and to quantify connectivity between lakes and groundwater. In particular, we evaluate if significant differences exist in the chemical composition of those water basins and if associated findings can shed light on the local surface and groundwater connectivity. We reach this goal by exploring the water quality of lakes (n=41) of archived datasets obtained from Environmental Impact Assessments (EIA) reports, and Crown-Indigenous Relations and Northern Affairs Canada (CIRNAC) and Kivalliq Inuit Association (KIA) annual field sampling reports. We demonstrate through statistical analyses that significant differences exist between the chemical composition of open taliks lakes and those with no taliks; although those differences are likely not entirely due to surface-groundwater interactions. Results also suggest that rock-water interactions can explain the chemical composition of waters in most of the lakes, but that some no open talik lakes are seemingly also affected by evaporation. We employ geochemical models to initially predict the chemical composition of open talik lakes once atmospherically equilibrated snow meltwaters have weathered local surficial deposits (i.e., till) and have subsequently mixed with hypersaline subpermafrost waters. A geochemical model is also utilized to model the predicted chemical evolution of no open talik lakes affected by evaporation. Our study reveals that we are lacking sufficient empirical data to properly predict which lakes have sublacustrine taliks below them and which do not. We conclude by proposing a list of additional measurements, data, and laboratory analyses that should be considered to better assess potential surface-groundwater interactions in the Rankin Inlet area.

TABLE OF CONTENTS

INTRODUCTION

A talik is a layer of unfrozen ground in a permafrost area (van Everdingen, 2005). In continuous permafrost regions, sublacustrine open (i.e., through) taliks occur mainly beneath large and deep lakes (> 2 m depth) that do not freeze to their bottom. In this context, the presence of open taliks and their hydrological connectivity with regional subpermafrost groundwater can have implications for the management of mine water inflow, thereby potentially affecting mine operations. Mining projects intersecting with open taliks can potentially affect lake water levels, lake water quality, and regional groundwater systems for water systems connected by these open taliks. Consequently, it is essential for mining projects to identify nearby lakes potentially underlain by open taliks and to understand the subpermafrost groundwater-surface flow dynamics. Although sublacustrine open taliks have been recognized as possible groundwater pathways, little is known about these open talik systems, their level of hydraulic connectivity, their residence time and the complex groundwater processes (temperature and density dependent) taking place (e.g., Kane et al., 2013; Morse, 2017).

In the field, sublacustrine open taliks can be detected via: 1) ground temperature measurements in deep boreholes ; and 2) ground or airborne electromagnetic surveys (see O'Neill et al., 2020, for a review on the subject). These approaches offer local assessment and/or are often expensive. Alternatively, the presence of sublacustrine open taliks, over a broad region, can be assessed using a 3D steady-state model of the thermal disturbance of lakes in permafrost environments (e.g., Burn, 2002). This model assumes that lakes are old enough for ground temperature beneath lakes to have reached an equilibrium state with the surrounding ground. Yet, to be reliable for a given location, the model must be fed with local data such as the deep geothermal gradient measured from ground temperatures. Validation of such approach, on a lake-by-lake basis, can be complex and expensive. Furthermore, the model is used to predict the presence or not of sublascustrine open taliks, but does not provide any indication on the level of their hydraulic connectivity with regional subpermafrost groundwater.

In continuous permafrost regions, we can expect that lake water chemistry is mainly dictated by climatic conditions (e.g., precipitation, evapoconcentration), near-surface processes (e.g., surface runoff, permafrost degradation) and weathering processes. However, one can suppose that the contribution from deep groundwater is also possible in presence of sublacustrine taliks assuming a certain level of hydraulic connectivity and supportive hydraulic gradient. Therefore, lake water chemistry can potentially serve as proxy data (and validation for thermal equilibrium modelling) for open talik detection and/or be used to infer groundwater contribution into lakes. Most of such surface water chemistry studies have mainly focused on groundwater contribution to streamflow in discontinuous permafrost environments (e.g., Cochand et al., 2019). In continuous permafrost environments, Dugan et al. (2012) used a radioactive isotope (^{222}Rn) with the goal to identify the presence of groundwater flow in a lake in the High Arctic, but results were not conclusive due to limited sampling locations within the lake. Larsen et al. (2017) used major cation concentrations to estimate groundwater inputs into 617 lakes in arctic and subarctic Alaska including 265 lakes in continuous permafrost areas. These basins were generally classified as thermokarst lakes without open taliks and conclusions on groundwater contribution to lakes were, therefore, limited to the discontinuous permafrost areas. Hinkel et al. (2016) studied thermokarst lakes with estimated subpermafrost groundwater contribution (via open taliks) and postulated that these lakes should have higher concentrations of mineral ions in solution than nearby lakes lacking an open talik. Their study site encompasses 28 lakes in an area of about 42,000km^2 on the North Slope of Arctic Alaska. In the geological context of their study, with few lakes spread across a broad region potentially influenced by different local factors and anthropogenic effects, the lakes suspected of having (or lacking) an open talik could not be discriminated in terms of their basic

hydrochemical characteristics. Although the latter studies proved to be non-conclusive, this does not prevent us from further exploring lake water chemistry as support data for open talik detection, especially for a geological context that differs from those mentioned above.

Lake water chemistry data (i.e., pH, specific conductivity, dissolved oxygen, major and trace ions concentrations) are commonly collected for Environmental Impact Assessment (EIA) purposes prior to the initiation of mining projects. The goal of this study is to take advantage of available archived data to determine if there are significant differences between the physical attributes and major solute composition of surface waters in lakes based on their potential connectivity with groundwater. Hence, to understand if basic limnological parameters can inform on surface-subsurface water interconnectivity in continuous permafrost environments. The study is proposed for the Rankin Inlet region where LeBlanc et al., (2022) classified lakes according to the potential presence (or absence) of sublacustrine open taliks below them. According to Golder (2016), the subpermafrost groundwater in the vicinity of the Agnico Eagle Meliadine Mine, near Rankin Inlet, is not connected to surface waters. This conclusion is driven by the fact that the main ion chemistry and isotope composition (δD-$\delta^{18}O$, tritium, strontium, and sulphate) of the groundwater is suggestive of a seawater origin with minimal to no component of surface water. However, the premise of the latter study is that lakes near the Agnico Eagle Meliadine Mine are likely only sources (and not sinks) of water for subpermafrost groundwaters. Hence, in the context of this investigation, we try to elucidate if surficial water bodies within the study area conversely act as sinks for groundwater flow and if its upward migration and lacustrine infiltration can be detected via analysis of basic limnological parameters in surficial waters.

STUDY AREA

Geology

The study area footprint is approximately 2,000 km^2, near the Hamlet of Rankin Inlet, Nunavut (62°48′35″ N, 92°5′58″ W) (**Figure 1**). The area is within the western Churchill Province of the Canadian Shield. The complex bedrock geology consists of the Archaean Rankin Inlet Greenstone Belt felsic volcanic rocks intercalated with mafic volcanic and sedimentary rocks, and granodioritic to tonalitic intrusions (Lawley et al., 2016). Regional east-west trending faults and other fault sets cut the fractured bedrock. The region was covered by the Laurentide Ice Sheet during the Wisconsin Glaciation and was free of ice by ~6 kyr BP (Dyke, 2004). The postglacial Tyrrell Sea extended as much as 150 km inland from the current coastline over the isostatically depressed land surface, reaching a maximum elevation of approximately 170 m above present sea level (Dyke, 2004; Randour et al., 2016). The surficial geology consists of glacial, marine, and glaciofluvial deposits, including eskers, with numerous bedrock outcrops (McMartin, 2002) that shape the topography with elevation raging from sea level to 300 m. The glacial deposits are unsorted to poorly sorted tills with a silty sand matrix.

Climate

The average mean annual air temperature (MAAT) for Rankin Inlet was −10.3°C from 1981–2020 with an average increase of 0.05°C/year (Environment and Climate Change Canada, 2022; **Figure 2**). Over the same period, the average annual total precipitation was 311 mm with no significant trends in total precipitation. The average total rain accounted for 184 mm whereas the average total snow was 131 cm. Prior to 1993, temperatures were below long-term average and rose above that average after 1993. The year 2010 was the warmest in the historical record and was followed by a cooling period consistent with the observed anomaly over the eastern Canadian Arctic region (Brown et al., 2018).

Permafrost

The region is situated within the continuous permafrost zone and permafrost thickness is generally 300 m near the coast and up to 500 m inland (Brown, 1963, 1978; Golder, 2014) while the depth of the basal cryopeg is estimated to be ~280-300 m below ground surface due to the groundwater salinity being ~1.8 times that of sea water (Golder, 2016). The geothermal gradient varies between 0.012 and 0.018 °C/m (Golder, 2014) while the mean annual ground temperature at the top of permafrost ranges between –9.5 and –5.5°C (LeBlanc & Oldenborger, 2021). The top of permafrost is ice rich in nearshore marine polygons and in poorly drained alluvial and marine sediments. Active-layer thickness ranges between 0.6–0.7 m in organic-rich alluvial-marine sediments and ~1.6 m in marine and organic-poor till deposits (LeBlanc & Oldenborger, 2021).

Water bodies

Kettle lakes and lakes shaped by glaciofluvial or glacial processes are common in the area (Golder, 2014), in contrast to thermokarst lakes. The glacial and glaciofluvial deposits are oriented in a northwest-southeast direction, which is also the preferential lake orientation (**Figure 1**). Lake (or pond) size ranges from 200 to 180 x 10^6 m² (Peter lake) with an average and median of 71,000 and 5,400 m², respectively. Maximum lake depths of about 100 surveyed lakes ranged from 0.11 to 23.5 m (Golder, 2012a, 2012b). Lake expansion and drainage due to warming climate since 1993 were attributed to thermokarst processes, observed in fine-grained and ice-rich sediments, and thickening of the active layer likely caused by the increase in subsurface water storage, in coarse-grained and ice-poor sediments, respectively (LeBlanc et al., 2020).

METHODS

Data

Water quality datasets related to hydroclimatic and hydrological parameters for the lakes, ponds, and groundwater in the vicinity of the Agnico Eagle Meliadine Mine area (**Figure 1**) were partially acquired from archived Final Environmental Impact Assessment (FEIA) and associated reports conducted by Golder Associates Ltd. (Golder, 2012a; 2012b; 2016), and Agnico Eagle Mines Ltd. (Agnico Eagle Mines Ltd., 2016). Archived limnological properties datasets were also obtained from Crown-Indigenous Relations and Northern Affairs Canada (CIRNAC) and the Kivalliq Inuit Association's (KIA) annual field sampling reports (CIRNAC-KIA, 2020). By combining those reports, we managed to acquire data on a total of 41 lakes and ponds situated within the Rankin Inlet area (**Table 1)**.

Only data collected prior to the Agnico Eagle Meliadine Mine's construction phase (i.e., year 2016 and prior) were considered in the study. Lakes and ponds for which we had multiple year of data were combined; the mean concentration is used in this study. Further, only measurements taken during the summer months (July or August) were considered in our assessment. Overall, only basic limnological properties (i.e., pH, specific conductivity, dissolved oxygen, and major ions loading) are used for this study; more often than not, this was the only data available for those water bodies.

Lake type classification

The presence (or absence) of open taliks below lakes/ponds situated within the vicinity of the Rankin Inlet region (and subsequent lake type classification) was inferred via a three-dimensional heat conduction and steady-state model of the thermal disturbance of lakes in periglacial landscapes. This model is provided in Burn (2002) and is based on the work of Lachenbruch (1957, 1959), Mackay (1962) and Smith (1976). Lake terrace width and maximum relative lake depth (for bottom-lake temperature prediction) were assessed for each lake, using remote-sensing optical imagery and high-resolution topographical data, which were included as input parameters in the model (LeBlanc et al., 2022). The other input parameter values are taken from Burn (2002), including values measured in the Rankin Inlet area (Golder, 2014). These values (i.e., geothermal gradient, mean annual ground temperature outside the lake, and lake terrace temperature) are non-unique but constrained by a range of possible values. The potential open talik class corresponds to lakes that meet the less severe thermal conditions (within the range of possible values) to have open talik beneath them (i.e., warmer lake terrace and surrounding ground and greater thermal gradient) whereas the open talik class corresponds to the more severe thermal conditions. Lakes that fall below the threshold of the less severe conditions are classified as no open talik.

Statistical analyses and machine learning

Statistical analyses were performed using the *R* open-source software. We first determined if there were significant statistic differences between open, potential, and no open talik lakes' median values for physicochemical properties by employing a Kruskal Wallis test because of the nonparametric nature of most of the distributions. The Kruskal Wallis was ran using the "pgirmess" package (Giraudoux, 2018). A multiple comparison Kruskal Wallis test was subsequently used to determine for which lake type median values were significantly different (i.e., higher than a critical value) at a significance level of 0.05.

A machine learning approach (i.e., unsupervised hierarchical clustering) was employed to create lake groupings according to their physicochemical characteristics (e.g., Ayenew et al., 2009). All inputs (i.e., pH, specific conductivities, TDS, and major ions loading) were rescaled with values ranging from -1 to 1 using the "Scale" built-in function in *R*. The "clValid" package (Brock et al., 2008) in *R* was used to determine which unsupervised machine learning algorithm should be used to divide lakes into groupings, and to assist in choosing the relevant number of clusters to use. This was done by assessing the connectivity, Silhouette Width, and Dunn Index internal measures.

Geochemical plotting and modelling

The Saturation Indices (SI) values in each water sample was calculated to provide insights into their source of solutes and helped in determining if the precipitation of secondary minerals may be limiting the concentration of various major ions (e.g., Obiefuna & Orazulike, 2011). SI for anhydrite, aragonite, calcite, dolomite, gypsum, halite and sylvite in the surface water samples were calculated using the PH REdox EQuilibrium (PHREEQC) hydrogeochemical program (Parkhurst & Appelo, 2013). SI values ≈ 0, < 0, and > 0 respectively indicate near equilibrium, undersaturated, and saturated solutions.

We also used a Gibbs diagram (Gibbs, 1970) to shed light on the mechanisms (i.e., rock-water interactions, atmospheric precipitation, evaporation) controlling the chemical composition of surface waters (e.g., Abadi Berhe et al., 2021; Asare-Donkor et al., 2018; Kaur et al., 2017). This is done by

plotting the TDS values for lentic basins of interest on the Y-axis and comparing them with ratios for main cations [Ca/(Ca+Na)] and anions [Cl/(Cl+HCO_3)].

The water samples' concentrations (mEq/L) in Ca^{2+} + Mg^{2+} vs. HCO_3^- + SO_4^{2-} were also compared to determine the origin of their solute load. This type of plot is commonly used to inform on the weathering regime to which surficial or groundwater samples are subjected to, and to evaluate if ion exchange (or reverse) reactions might be limiting or augmenting the load of specific ions (e.g., Fisher & Mullican, 1997; Gopinath et al., 2019; Kaur et al., 2017; Tamma Rao et al., 2015). Samples plotting above the 1:1 equiline are expected to have their chemical composition mostly affected by carbonate dissolution while on the contrary, those plotting below the 1:1 equiline would have a hydrochemical facies imputable to silicate weathering. The Na^+-normalized molar concentrations of Mg^{2+} vs. Ca^{2+} were also plotted to a predict the respective roles that carbonate and silicate weathering (as well as the dissolution of evaporites) have on the solute load of water samples (Gaillardet et al., 1999). Waters that have dissolved large amounts of evaporatites tend to have Mg^{2+}/ Na^+ and Ca^{2+}/ Na^+ ratios close to 0.01 and 0.1, respectively. On the other hand, silicate mineral enriched waters will have Mg^{2+}/ Na^+ and Ca^{2+}/ Na^+ ratios of ~1 whereas waters enriched in dissolved carbonates will have the highest ratios (i.e., ~ 10 and ~ 100 for Mg^{2+}/ Na^+ and Ca^{2+}/ Na^+, respectively).

Numerical modelling for geochemical interactions (i.e., weathering) between surface waters and local surficial deposits was undertaken with the PHREEQC program (e.g., Faucher et al., 2021; Marsh et al., 2020). Results from the weathering simulations provide first-order estimations on the predicted major ions loading (and thereby relative concentration) of surface waters in the Rankin Inlet region if weathering of local surficial deposits is their main or only source of solute. We performed weathering simulations using atmospherically equilibrated (pCO_2 = -3.43 atmospheres) snow meltwater sampled at the nearby Saqvaqjuac research site (Welch & Legault, 1986) and given that most of the open talik lakes in the area (for which we have data) sit on glacial diamicton deposits, we chose to interact this initial water source with various mineralogical assemblages of local greenstone- and granite-rich till deposits (McMartin, 2000). The open-system weathering simulations of the greenstone (i.e., chlorite, plagioclase, illite, amphibole) and granitic (i.e., quartz, k-feldspar, plagioclase, illite, amphibole) mineral assemblages (or a mix of both) were ran with and without the addition of carbonate (i.e., calcite, dolomite) minerals. Then, a two-component mixing (i.e., surface and groundwater) was also undertaken in PHREEQC using the hydrochemical properties of subpermafrost groundwaters sampled at the Agnico Eagle Meliadine Mine and the outputs of the weathering simulations earlier described.

The influence of evaporative processes on the major solute load and pH of no open talik lakes (i.e., evapoconcentration) was modelled using the PHREEQC program. We inferred that the initial (i.e., prior to being affected by evaporative processes) chemical composition of no open talik lakes would likely resemble that of Lake Meliadine, a nearby large open talik lake affected to a much lesser degree by vaporization of liquid water. The model predicts the molalities of major ions in the residual water and solid molalities of precipitated secondary minerals (i.e., calcite, gypsum, anhydrite, and halite) at various concentration factors. The concentration factor (CF=1/residual water content) was multiplied by 2 at each step, until a CF was equal to 32 (or 3.1% of residual water content), and simulations were using initial pCO_2 values of $10^{-3.43}$ and $10^{-3.00}$ atmospheres to mimic waters either in equilibrium with the atmosphere or slightly more acidic.

RESULTS AND DISCUSSION

Physicochemical properties of lakes/ponds in the region of interest

The regional assessment of the presence of sublacustrine taliks below lentic basins in the area (LeBlanc et al., 2022) suggests that five, nine, and twenty-seven of the 41 lakes and ponds, extracted from available reports, can respectively be classified as open talik, potential open talik, and no open talik lakes/ponds (**Table 1**).

The pH values in lakes predicted to have potential surface-groundwater interactions via sublacustrine taliks (i.e., open talik lakes) are circumneutral and fluctuate from 6.8 to 7.4 (**Table 2; Figure 3**). The waters' specific conductivity and dissolved oxygen content vary from 37 to 77 $\mu S/cm^{-1}$ and from 91 to 124 % saturation, respectively. Surface water from lakes identified as open talik lakes have a Ca-HCO_3 hydrochemical facies (**Figure 4**) with Ca^{2+} and HCO_3^- concentrations varying from 0.16 to 0.36 and 0.18 to 0.36 mEq/L, respectively (**Figure 5**). Their Total Dissolved Solids (TDS) load ranges from 16 to 35 ppm, and based on the available data concerning total phosphorus and chlorophyll-α levels, those can be classified as oligotrophic basins (Nürnberg, 1996).

In lakes classified as potential open talik lakes, pH values are also circumneutral and vary from 6.7 to 7.8. The specific conductivity and dissolved oxygen content range from 50 to 230 $\mu S/cm^{-1}$ and from 92 to 115 % saturation, respectively. All but one potential open talik lakes (i.e. Nipissar Lake) have a Ca-HCO_3 hydrochemical facies. The latter has a Na(Ca)-Cl facies. The Ca^{2+} and HCO_3^- content in potential open talik lakes varies from 0.23 to 0.80 mEq/L and 0.26 to 0.76 mEq/L, respectively. Concentrations in Na^+ and Cl^- alternate from 0.09 to 0.83 mEq/L and from 0.12 to 0.87 mEq/L, whereas the range of their TDS load is between 31 and 150 ppm, respectively. Total phosphorus and chlorophyll-α levels are within the oligotrophic to mesotrophic range (Nürnberg, 1996).

Surface water samples taken from the no open talik lakes have circumneutral to slightly basic pH values (6.7 to 8.5). The range for specific conductivity and dissolved oxygen content values is from 48 to 1,695 $\mu S/cm^{-1}$ and from 91 to 121 %, respectively. Their TDS load fluctuates from 29 to 1440 ppm. No open talik basins with the highest TDS loading have a Ca-Cl hydrochemical facies, and those with fresher surface waters have Ca(Na)-Cl or Ca-HCO_3 facies. Concentrations in Ca^{2+} and HCO_3^- ions are within the range of 0.31 to 19.57 mEq/L and from 0.04 to 2.47 mEq/L, respectively. Their Na^+ and Cl^- loading ranges from 0.02 to 2.35 mEq/L and from 0.06 to 24.96 mEq/L, respectively. Nutrient levels in those surface water samples (i.e., total phosphorus and chlorophyll-α) imply that no open talik lakes within the Rankin Inlet area are either oligotrophic or mesotrophic (Nürnberg, 1996).

The Kruskal-Wallis rank-sum test suggests that there are significant differences between lake type distribution in terms of median values for some of their physicochemical properties (**Table 2**). Yet, results from this statistical analysis provide a line of evidence that dissolved oxygen content, Cl^- concentration, and Cl^- normalized ratios are not significantly different between basins classified as open talik, no open talik, and potential open talik lakes.

The multiple comparison test after Kruskal-Wallis (**Table 3**) demonstrates that median specific conductivities in surface water samples are only significantly different between open talik and no open talik lakes. Median TDS loading values are significantly different between the open talik vs. no open talik lakes, and potential open talik vs. no open talik lakes. Significant differences in terms of median pH values exist between open talik vs. no open talik and potential open talik vs. no open talik lakes. Results also show that median surface water concentrations in Ca^{2+}, Mg^+, SO_4^{2-}, and HCO_3^- are

significantly different between open talik vs. no open talik and potential open talik vs. no open talik lakes. Conversely, the only significant difference regarding Na^+ loading in Rankin Inlet lakes is between potential open talik and no open talik basins.

Establishing lake groupings according to physicochemical properties

An unsupervised machine learning hierarchical clustering analysis of the Rankin Inlet area's lentic basins' physicochemical properties demonstrates that lakes should be divided into two distinct groupings (i.e., clusters) (**Figure 6**). The first cluster is composed of five no open talik lakes. The second group (n=36) encompasses open, no open and potentially open talik lakes seemingly sharing enough in common to be joined together. The mean pH values (7.98) in lakes of cluster #1 are slightly higher than for those in the second cluster (7.66) (**Table 4**). In water samples of cluster #1, mean specific conductivities alongside mean TDS are much higher (1418 $\mu S/cm^{-1}$ and 876 ppm) compared to those of cluster #2 (140 $\mu S/cm^{-1}$ and 82 ppm). In addition, mean major ions concentrations in the cluster #1 basins were 13.47, 14.83, 2.32, 1.32, 0.49, 1.04 mEq/L for Ca^{2+}, Cl^-, Mg^{2+}, Na^+, SO_4^{2-}, and HCO_3^-, respectively. Mean loading values for the previously enumerated major ions in cluster #2 were 0.81, 0.45, 0.19, 0.20, 0.05, and 0.67 mEq/L. Thus, when basic physicochemical properties are solely employed, we are left with surface water body samples either much more enriched in water-soluble salts and with a relatively high pH (cluster #1) compared to their counterparts in cluster #2. This discrepancy in terms of pH and solute ion loading for those five no open talik basins is likely caused by evapoconcentration of solutes. We explore this hypothesis via evaporation modelling further in this report.

Source of solutes

When plotted on a Gibbs diagram (**Figure 7**), open talik lakes fall between the precipitation and rock dominance zones. This is also the case for potential open talik lakes, with the exception of Nipissar Lake. The latter plots higher on the Y-axis (due to its higher TDS load) within the rock dominance zone. Results also provide hints that the no open talik lakes within the Rankin Inlet area are all affected by rock-water interactions (i.e., weathering). Nonetheless, when comparing TDS values with dominant anions ratios, it is also apparent that rainfall (surficial lacustrine water in this case) evaporation seems to play a role in the major ion solute enrichment of many no open talik lakes. Considering that rock-water interactions are affecting the chemical composition of most of the lentic basins of interest, an evaluation of the relative contribution of either silicate or carbonate weathering/dissolution (or a mix of both) should be made to gauge how weathering of surficial geological units alone might be influencing the solute loading of those lakes and ponds. We have done so by first comparing the water samples' concentrations (mEq/L) in $Ca^{2+} + Mg^{2+}$ vs. $HCO_3^- + SO_4^{2-}$ (**Figure 8A)**. Once plotted, surficial water samples mostly fall above or along the 1:1 equiline: an indication of a mixed influence of carbonate and silicate weathering on the surficial water samples' chemistry, with carbonate weathering seemingly having a larger influence on most of the lentic basins (especially the no open talik lakes).

Further, the comparison of Na^+ normalized molar concentrations of Mg^{2+} vs. Ca^{2+} (**Figure 8B)** provides a line of evidence that a mix of silicate and carbonate weathering likely affects those surficial water samples. Those results also imply that the dissolution of evaporite minerals is not a controlling factor on their hydrochemistry. According to Tella et al. (2005), lakes of interest in the Rankin Inlet area are encased in either Quaternary diamicton or bedrock units. Those are both partially composed of silicate and (to a lesser extent) carbonate minerals (Lawley et al., 2016; McMartin, 2000), meaning that the chemical weathering of those local geological units presumably be a source of major dissolved ions in the lentic basins of the area.

Predicting the chemical composition of open talik lakes using a two-component mixing approach

Under a two-component mixing model of weathering simulation outputs and groundwaters (**Figure 9; Table A1**), it first appears that pH in the open talik lakes can only be somewhat obtained when the greenstone (simulation #5) and granitic (simulation #6) equilibrated waters, individually (and without carbonates), are mixed with 10% of subpermafrost groundwaters. Weathering simulations alone yield higher (i.e., simulations #1-3) or lower (simulations #4-6) Ca^{2+}/Cl^- compared to open talik lakes. Nonetheless, this ratio for open talik lakes is reached when output waters from simulations #1-3 and #4-6 are mixed with <1% and >10% of volume with subpermafrost groundwater, respectively. The best fit for open talik lakes' Na^+/Cl^- ratios solely using weathering simulation results is achieved with those that do not include carbonates (i.e., simulations #4-6). Yet, Na^+/Cl^- ratios in open talik lakes can be reached with simulations #1-3 once a minimal amount (~ 1%) of groundwater gets added in the two-component mixing scheme. Finally, the closest we can get to HCO_3^-/Cl^- Specific conductivity and dissolved oxygen content values within those lentic basins range thermodynamic equilibrium with the mineralogy of the local granite-rich till. Otherwise, this ratio is only reached with other weathering simulations once they are mixed with <1% of mixing volume with subpermafrost groundwater.

Evapoconcentration of solutes and effects on lacustrine hydrochemical facies

The unsupervised machine learning clustering of Rankin Inlet's lentic basins (**Figure 6**) demonstrates that five of those stand out in terms of their chemical composition: those no open talik basins' surficial water samples have a higher pH and TDS load compared to waters in other basins. Further, as previously demonstrated, statistical analysis of the major ions loading between lake types provides a line of evidence that no open talik lakes/ponds generally have significantly saltier waters than potential and open talik basins. This is somewhat surprising since it is often presumed that open talik lakes connected to hypersaline groundwaters should display higher TDS load and specific conductivity (e.g., Hinkel et al., 2017) than no open talik lakes. Yet, in the case of Rankin Inlet's basins, we truly see an opposite trend.

The sublacustrine talik configuration assessment made by LeBlanc et al. (2022) for Rankin Inlet area's lakes relies heavily on surface area and water column depth measurements. By use of this classification scheme, small lakes (or ponds) with shallow water columns are typically classified as no open talik lakes. Moreover, it has been well established that morphometric properties (i.e., surface area, water column depth and associated volume) of lentic basins have a great impact on evaporation rates (e.g., Deng et al., 2013; Subin et al., 2012; Xiao et al., 2018): the smaller the lentic basins, the more pronounced the influence of evaporation of the concentration of solutes will be on its chemical composition. We therefore hypothesize that the high solute load (and pH) in no open talik lakes is partially imputable to the enhanced effect that evaporation has on those water bodies (accompanied by lesser input contributions from atmospheric precipitations and active layer thawing), compared to bigger basins (e.g., open talik lakes) (**Table 1**). This is supported by the negative correlation between surface area and salinity for no open talik lakes. (**Figure 10**).

Results from our evaporation simulations (**Table 5**) match reasonably well the empirical data concerning predicted pH and HCO_3^- in no open talik basins if evaporation is indeed removing most of its water content (**Figure 11**). The evaporation hypothesis is also supported by the aragonite and calcite SI values (**Table A2**) of many no open talik lakes (including those five classified in group #1 via hierarchical clustering) that have a relatively higher TDS load and pH than others. For example, our evaporation model demonstrates that calcite may become oversaturated in surficial waters once ~75% of the basins'

initial water content (CF~4) has been evaporated. Results also demonstrate quite well the effect of evaporation of the concentration of dissolved solutes in such water bodies.

Still, although our evaporation simulations explain the measured bicarbonate load and pH in no open talik lakes predicted to be substantially influenced by evaporation, our evaporation model does not provide a viable explanation as to why those solute enriched basins also exhibit a Ca-Cl hydrochemical facies. Under evaporation (and using Lake Meliadine's water composition for our inputs), our model predicts that up to a CF of 32, the only evaporite minerals that should form should be of calcium carbonate type (i.e., aragonite or calcite). The precipitation of calcium carbonates should subsequently remove Ca^{2+} and HCO_3^-, and conversely augment the concentration of remaining major ions. Consequently, our model predicts that overtime, a transformation from an initial Ca-HCO_3 to a Na-Cl hydrochemical facies should occur in evaporation-affected no open talik basins (**Figure 12**). In spite of the fact that a Cl^- concentration increase in evaporation-affected basins does seem to take place, we see an opposite trend with Ca^{2+} content, where solute enriched lakes/ponds are relatively more enriched in Ca^{2+} than other lakes with a lower TDS loading. It follows that besides evaporation, at least another phenomenon is seemingly altering their chemical composition.

Recent local mining activities have seemingly not caused waters in those no open talik basins to deviate from a typical Ca-HCO_3 and shift towards a Ca-Cl hydrochemical facies. The all-weather access road between the Meliadine Mine and Rankin Inlet was constructed between 2013 and 2014, and sampling undertaken in 2007 (Golder, 2012a) demonstrates that even at the time, their water column had a Ca-Cl chemical signature. Hence, anthropogenic activities (i.e., mining) can reasonably be ruled out. Instead, one plausible avenue capable of explaining the odd Ca-Cl hydrochemical facies in surficial waters of some no open talik basins enriched in solutes and with slightly basic pH values could be via reverse ion exchange reactions. Experiments performed by (Beekman & Appelo, 1990) demonstrated using column experiments that Na^+ may be exchange to Ca^{2+} in a solution where freshwater is mixed with saltwater diluted 1:1 with distilled water. This chemical reaction is rather common is groundwaters (Zaidi et al., 2015). The Rankin Inlet area was submerged by the Tyrell sea during the last deglaciation (Dyke, 2004) and laid down marine deposits throughout the area (McMartin, 2002). Once eroded and/or leached, those marine deposits could provide a source of Ca^{2+} enriched clays and brines. Once mixed with fresh surficial waters, such exchange of Na^+ (from the no open talik lakes) for Ca^{2+} (in the marine deposits leachate) could hypothetically occur, thereby shifting values towards the left in a cationic ternary diagram. This hypothesis is also supported by a comparison between the no open talik basins' Ca^{2+} + Mg^{2+} vs. HCO_3^- + SO_4^{2-} loading (**Figure 8A)**. Reverse cation exchange processes can shift points above (left of) the 1:1 equiline (e.g., Rajmohan & Elango, 2004; Zaidi et al., 2015) and this is observed with many of the no open talik lakes.

CONCLUSION

We assessed if there were any significant differences between the physicochemical characteristics in surficial water samples of lentic basins situated in the Rankin Inlet area classified according to the potential occurrence of a sublacustrine talik below them (i.e., open talik, potential open talik and no open talik lakes). Based on our results, the following five conclusions can be reached:

1) Statistical analyses reveal that significant differences exist between the hydrochemical composition of open, no open and potential open talik basins (especially between open and no open talik basins). In general, no open talik water bodies have a much higher solute load and slightly higher pH than open talik lakes, whereas potential open talik lakes fall in between.

Further, unlike most water bodies for which we had data, no open talik lakes with a high solute load and pH hosted Ca-Cl type waters (vs. Ca-HCO_3).

2) An unsupervised machine-learning algorithm proposes to divide the 41 lakes/ponds into two groupings in relation to their major ions loading, pH, and specific conductivities. The first cluster contains five no open talik water bodies with a high solute load, specific conductivity and pH; all other lakes are grouped in the second cluster. Thus, those basic hydrochemical properties alone cannot serve to differentiate water bodies in the Rankin Inlet area with regard to predicted surficial-groundwater interactions.

3) Rock-water interactions can explain the chemical composition of waters in open and potential open talik lakes. The no open talik lakes have a chemical composition affected by rock-water interactions and evaporation. Further, a two-component mixing model between waters equilibrated with local mineral assemblages and subpermafrost meltwaters fails to match empirical data concerning the chemical composition of open talik water bodies. This is unfortunate but unsurprising since the chemical composition of open talik lakes in periglacial landscapes results from complex synergetic surface and subsurface interactions (e.g., Dugan et al., 2012; Hinkel et al., 2017). This means that the chemical weathering of surficial geological deposits is likely not the only source of sub-aerial solutes. This exercise should be repeated using a multiple-component end-member mixing model (Koch et al., 2014; Li et al., 2020; Lu et al., 2008), once we will have gathered additional geochemical data on those likely sources (e.g., permafrost degradation, surface runoff, leaching of marine sediments) and on the chemical composition of bottom lake waters.

4) We demonstrated using an evaporative model that, through time, evapoconcentrated lakes (i.e., small no open talik basins) should evolve towards a Na-Cl hydrochemical facies and precipitate calcium carbonates, resulting in an increase in pH. Yet, no open talik lakes with a high pH and solute load have Ca-Cl type waters. We do not have a definitive explanation for the cause of this odd Ca-Cl hydrochemical signature and propose that reverse cation exchanges could one of the underlying cause(s).

5) We are lacking sufficient empirical data to predict which basins have sublacustrine taliks below them and which do not (i.e., to validate LeBlanc et al.'s (2022) model). Below is a list of additional measurements, data, and laboratory analyses that should be considered in order to better assess potential surface-groundwater interactions in the Rankin Inlet area. Once acquired and taken into account in our comparative assessment of hydrochemical properties, this additional data should be much more useful and informative for sublacustrine open talik prediction than what was used for the above study:

    -Water column depth profile physicochemical measurements (i.e., temperature, pH, specific conductivity, dissolved oxygen content) in lakes/ponds of different types.

    -Stable water isotope (δD-$\delta^{18}O$) analysis with depth (i.e., every x meters) of the basins' water column.

    -Geochemical analysis (i.e., major and trace ions) with depth of the basins' water column.

-Characterization of Dissolved Inorganic and Organic Carbon (DIC-DOC) including stable carbon isotope ratios (i.e., $\delta^{13}C_{DIC}$- $\delta^{13}C_{DOC}$) with depth in the lakes/ponds' water column.

-Dating ($^{14}C_{DIC}$-$^{14}C_{DOC}$ and ^{3}H) of lake water column and subpermafrost groundwater samples at various depths.

-Determination of dissolved noble gas (Ne, Ar, Kr, Xe) concentrations (and ratios) via passive diffusion sampling at varying depths in lentic water bodies of interest.

-Collection of hydrogeological data (e.g., bedrock geology, location of fractures and fault systems, determination of the direction of hydraulic gradients away or towards lakes).

ACKNOWLEDGEMENTS

This study was funded by the Natural Resources Canada's GEM-GeoNorth program. We are greatful to the Crown-Indigenous Relations and Northern Affairs Canada (CIRNAC) and Kivalliq Kivalliq Inuit Association (KIA) for allowing us to consult and use their archived limnological datasets in the context of this study. Many thanks to Sarah Forté for providing the latter dataset. We would also like to extend our gratitude to the reviewer, Nicolas Benoit, for his constructive comments and suggestions.

REFERENCES

Abadi Berhe, B., Woldemariyam Tesema, F., & Mebrahtu, G. (2021). Assessment of Major Sources Controlling Groundwater Chemistry in Kombolcha Plain, Eastern Amhara Region, Ethiopia. *Momona Ethiopian Journal of Science*, *13*(1), 21–42. https://doi.org/10.4314/mejs.v13i1.2

Agnico Eagle Mines Ltd. (2016). *MELIADINE GOLD PROJECT 2016 Annual Report; unpublished report*.

Asare-Donkor, N. K., Ofosu, J. O., & Adimado, A. A. (2018). Hydrochemical characteristics of surface water and ecological risk assessment of sediments from settlements within the Birim River basin in Ghana. *Environmental Systems Research*, *7*(1), 1–17. https://doi.org/10.1186/s40068-018-0113-1

Ayenew, T., Fikre, S., Wisotzky, F., Demlie, M., & Wohnlich, S. (2009). Hierarchical cluster analysis of hydrochemical data as a tool for assessing the evolution and dynamics of groundwater across the Ethiopian rift. *International Journal of Physical Sciences*, *4*(2), 076–090.

Beekman, H. E., & Appelo, C. A. J. (1990). Ion chromatography of fresh- and salt-water displacement--laboratory experiments and multicomponent transport modelling. *Journal of Contaminant Hydrology*, *7*, 21–37.

Brock, G., Phillur, V., & Datta, S. (2008). clValid: An R Package for Cluster Validation. *Journal of Statistical Software*, *25*(4), 1–22.

Brown, R., Barrette, C., Brown, L., Chaumont, D., Grenier, P., Howell, S., & Sharp, M. (2018). Climate variability, trends and projected change. In T. Bell & T. M. Brown (Eds.), *Chapter 2 in From Science to Policy in the Eastern Canadian Arctic: an Integrated Regional Impact Study (IRIS) of Climate Change and Modernization* (ArcticNet, p. 38).

Brown, R. J. E. (1963). Relation between mean annual air and ground temperatures in the permafrost region of Canada. *Proceedings of the First International Conference on Permafrost, Lafayette, Indiana, November 11–15*, 241–246.

Brown, R. J. E. (1978). Influence of climate and terrain on ground temperatures in the continuous permafrost zone of northern Manitoba and Keewatin district, Canada. *Proceedings of the Third International Conference on Permafrost, Edmonton, Alberta, July 10–13*, 15–22.

Burn, C. R. (2002). Tundra lakes and permafrost, Richards Island, Western Arctic coast, Canada. *Canadian Journal of Earth Sciences*, *39*(8), 1281–1298. https://doi.org/10.1139/e02-035

CIRNAC-KIA. (2020). *Annual field sampling reports (2005-2019)*.

Cochand, M., Molson, J., & Lemieux, J. M. (2019). Groundwater hydrogeochemistry in permafrost regions. *Permafrost and Periglacial Processes*, *30*(2), 90–103. https://doi.org/10.1002/ppp.1998

Deng, B., Liu, S., Xiao, W., Wang, W., Jin, J., & Lee, X. (2013). Evaluation of the CLM4 lake model at a large and shallow freshwater lake. *Journal of Hydrometeorology*, *14*(2), 636–649. https://doi.org/10.1175/JHM-D-12-067.1

Dugan, H. A., Gleeson, T., Lamoureux, S. F., & Novakowski, K. (2012). Tracing groundwater discharge in a High Arctic lake using radon-222. *Environmental Earth Sciences*, *66*(5), 1385–1392. https://doi.org/10.1007/s12665-011-1348-6

Dyke, A. S. (2004). An outline of North American deglaciation with emphasis on central and northern Canada. *Developments in Quaternary Sciences*, *2*, 373–424.

Environment and Climate Change Canada. (2022). *Historical climate data; Environment and Climate Change Canada, URL <http://climate.weather.gc.ca/>. [January 2022]*.

Faucher, B., Lacelle, D., Marsh, N. B., Fisher, D. A., & Andersen, D. T. (2021). Ice-covered ponds in the Untersee Oasis (East Antarctica): Distribution, chemical composition, and trajectory under a warming climate. *Arctic, Antarctic, and Alpine Research*, *53*(1), 324–339. https://doi.org/10.1080/15230430.2021.2000566

Fisher, R. S., & Mullican, F. W. (1997). Hydrochemical evolution of sodium-sulfate and sodium-

chloride groundwater beneath the Northern Chihuahuan Desert, Transpecos, Texas, U.S.A. *Journal of Hydrogeology*, *5*, 14–16.

Gaillardet, J., Dupre, B., Louvat, P., & Allegre, C. J. (1999). Global silicate weathering and CO consumption rates deduced from the chemistry of large rivers. *Chemical Geology*, *159*(8), 3–30.

Gibbs, R. J. (1970). Mechanisms Controlling World Water Chemistry. *Science*, *170*(3962), 1088–1090.

Giraudoux, P. (2018). *Pgirmess: Spatial Analysis and Data Mining for Field Ecologists*.

Golder. (2012a). *SD 7-1 Aquatics Baseline Synthesis Report, 1994 to 2009 - Meliadine Gold Project, Nunavut – Meliadine Gold Project; unpublished report prepared by Golder Associates Ltd. for Agnico-Eagle Mines Limited, Doc 327-1013730076 Ver. 0*.

Golder. (2012b). *SD 7-2 2011 Aquatic Baseline Studies - Meliadine Gold Project, Nunavut – Meliadine Gold Project; unpublished report prepared by Golder Associates Ltd. for Agnico-Eagle Mines Limited, Doc 246-1013730076 Ver. 0*. 77.

Golder. (2014). *SD 6-1 permafrost thermal regime baseline studies – Meliadine Gold Project; unpublished report prepared by Golder Associates Ltd. for Agnico-Eagle Mines Limited, Doc 225-1314280007 Ver. 0.*

Golder. (2016). *Surface Water and Groundwater Quality Investigation in Support of the Underground Mine Development at Tiriganiaq – Meliadine Gold Project; unpublished report prepared by Golder Associates Ltd. for Agnico-Eagle Mines Limited, Doc 555-1416135 1803_16 Ver 0*.

Gopinath, S., Srinivasamoorthy, K., Saravanan, K., & Prakash, R. (2019). Discriminating groundwater salinization processes in coastal aquifers of southeastern India: geophysical, hydrogeochemical and numerical modeling approach. *Environment, Development and Sustainability*, *21*(5), 2443–2458. https://doi.org/10.1007/s10668-018-0143-x

Hinkel, K. M., Arp, C. D., Townsend-Small, A., & Frey, K. E. (2016). Can Deep Groundwater Influx be Detected from the Geochemistry of Thermokarst Lakes in Arctic Alaska? *Permafrost and Periglacial Processes*, *28*(3), 552–557. https://doi.org/10.1002/ppp.1895

Kane, D. L., Yoshikawa, K., & McNamara, J. P. (2013). Regional groundwater flow in an area mapped as continuous permafrost, NE Alaska (USA). *Hydrogeology Journal*, *21*, 41–52.

Kaur, T., Bhardwaj, R., & Arora, S. (2017). Assessment of groundwater quality for drinking and irrigation purposes using hydrochemical studies in Malwa region, southwestern part of Punjab, India. *Applied Water Science*, *7*(6), 3301–3316. https://doi.org/10.1007/s13201-016-0476-2

Koch, J. C., Kikuchi, C. P., Wickland, P., & Schuster, P. (2014). Runoff sources and flow paths in a partially burned, upland boreal catchment underlain by permafrost. *Water Resources Research*, 5375–5377. https://doi.org/10.1002/2013WR014979.Reply

Lachenbruch AH. (1957). Three-dimensional heat conduction beneath heated buildings. *United States Geological Survey Bulletin 1052-B*, 51–69.

Lachenbruch AH. (1959). Periodic heat flow in a stratified medium with application to permafrost problems. *United States Geological Survey Bulletin 1083-A:*, 1–36.

Larsen, A. S., O'Donnell, J. A., Schmidt, J. H., Kristenson, H. J., & Swanson, D. K. (2017). Physical and chemical characteristics of lakes across heterogeneous landscapes in arctic and subarctic Alaska. *Journal of Geophysical Research: Biogeosciences*, *122*(4), 989–1008. https://doi.org/10.1002/2016JG003729

Lawley, C. J. M., McNicoll, V., Sandeman, H., Pehrsson, S., Simard, M., Castonguay, S., Mercier-Langevin, P., & Dubé, B. (2016). Age and geological setting of the Rankin Inlet greenstone belt and its relationship to the gold endowment of the Meliadine gold district, Nunavut, Canada. *Precambrian Research*, *275*, 471–495. https://doi.org/10.1016/j.precamres.2016.01.008

LeBlanc, A.-M., Bellehumeur-Génier, O., Oldenborger, G. A., & Short, N. (2020). Lake area and shoreline changes due to climate and permafrost-related drivers, Rankin Inlet area, Nunavut. *Summary of Activities 2019, Canada-Nunavut Geoscience Office*, 79–92.

LeBlanc, A.-M., Chartrand, J., & Smith, S. L. (2022). *Regional assessment of the occurrence of taliks below Arctic lakes. Geological Survey of Canada Scientific Presentation 138.* https://doi.org/10.4095/330205''

LeBlanc, A.-M., & Oldenborger, G. A. (2021). Ground temperature, active-layer thickness and ground-ice conditions in the vicinity of Rankin Inlet, Nunavu. *Summary of Activities 2020, Canada-Nunavut Geoscience Office*, 63–72.

Li, Z. J., Li, Z. X., Fan, X. J., Wang, Y., Song, L. L., Gui, J., Xue, J., Zhang, B. J., & Gao, W. De. (2020). The sources of supra-permafrost water and its hydrological effect based on stable isotopes in the third pole region. *Science of the Total Environment*, *715*, 136911. https://doi.org/10.1016/j.scitotenv.2020.136911

Lu, G., Sonnenthal, E. L., & Bodvarsson, G. S. (2008). Multiple component end-member mixing model of dilution: Hydrochemical effects of construction water at Yucca Mountain, Nevada, USA. *Hydrogeology Journal*, *16*(8), 1517–1526. https://doi.org/10.1007/s10040-008-0322-1

Mackay, J. R. (1962). Pingos of the Pleistocene Mackenzie Delta area. *Geographical Bulletin*, *18*, 21–63.

Marsh, N. B., Lacelle, D., Faucher, B., Cotroneo, S., Jasperse, L., Clark, I. D., & Andersen, D. T. (2020). Sources of solutes and carbon cycling in perennially ice-covered Lake Untersee, Antarctica. *Scientific Reports*, *10*(1), 1–12. https://doi.org/10.1038/s41598-020-69116-6

McMartin, I. (2000). *Till composition across the Meliadine Trend, Rankin Inlet Area, Kivalliq region, Nunvavut. Geological Survey of Canada, Open File 3747.*

McMartin, I. (2002). *Surficial geology, Rankin Inlet, Nunavut; Geological Survey of Canada, Open File 4116, scale 1:50 000,.*

Morse, P. (2017). *Report on the Permafrost and Hydrogeology Interactions meeting, 14 November 2016, Yellowknife, NWT; Geological Survey of Canada, Open File 8192, 60 p. (also Northwest Territories Geological Survey, NWT Open Report 2017-010). doi:10.4095/299674*.

Nürnberg, G. K. (1996). Trophic state of clear and colored, soft- and hardwater lakes with special consideration of nutrients, anoxia, phytoplankton and fish. *Lake and Reservoir Management*, *12*, 432–447.

O'Neill, H. B., Roy-Leveillee, P., Lebedeva, L., & Ling, F. (2020). Recent advances (2010–2019) in the study of taliks. *Permafrost and Periglacial Processes*, *31*(3), 346–357. https://doi.org/10.1002/ppp.2050

Obiefuna, G. I., & Orazulike, D. M. (2011). The Hydrochemical Characteristics and Evolution of Groundwater in Semiarid Yola Area , Northeast , Nigeria. *Research Journal of Environmental and Earth Sciences*, *3*(4), 400–416.

Parkhurst, D. L., & Appelo, C. A. J. (2013). Description of Input and Examples for PHREEQC Version 3 — A Computer Program for Speciation , Batch-Reaction , One-Dimensional Transport , and Inverse Geochemical Calculations. In *U.S. Geological Survey Techniques and Methods, book 6, chapter A43*. https://doi.org/10.1016/0029-6554(94)90020-5

Pavlova, N., Lebedeva, L., & Efremov, V. (2019). Lake water and talik groundwater interaction in continuous permafrost, Central Yakutia. *E3S Web of Conferences*, *98*. https://doi.org/10.1051/e3sconf/20199807024

Rajmohan, N., & Elango, L. (2004). Identification and evolution of hydrogeochemical processes in the groundwater environment in an area of the Palar and Cheyyar River Basins, Southern India. *Environmental Geology*, *46*(1), 47–61. https://doi.org/10.1007/s00254-004-1012-5

Randour, I., Mcmartin, I., & Roy, M. (2016). *Study of the postglacial marine limit between Wager Bay and Chesterfield Inlet , western Hudson Bay , Nunavut*. *December*, 51–60.

Smith, M. W. (1976). *Permafrost in the Mackenzie delta, Northwest Territories. Geological Survey of Canada, Paper 75-28.*

Subin, Z. M., Riley, W. J., & Mironov, D. (2012). An improved lake model for climate simulations:

Model structure, evaluation, and sensitivity analyses in CESM1. *Journal of Advances in Modeling Earth Systems*, *4*(2), 1–27. https://doi.org/10.1029/2011MS000072

Tamma Rao, G., Srinivasa Rao, Y., Mahesh, J., Surinaidu, L., Ratnakar, D., Gurunadha Rao, G., & Durga Prasad, M. (2015). Hydrochemical assessment of groundwater in alluvial aquifer region, Jalandhar District, Punjab, India. *Environmental Earth Sciences*, *73*(12), 8145–8153. https://doi.org/10.1007/s12665-014-3973-3

Tella, S., Paul, D., Davis, W. J., Berman, R. G., Sandeman, H. A., Peterson, T. D., Pehrsson, S. J., & Kerswill, J. A. (2005). *Bedrock geology compilation and regional synthesis, parts of Hearne domain, Nunavut. Geological Survey of Canada, Open File 4729.*

van Everdingen, R. O. (2005). Multi-language glossary of permafrost and related ground-ice terms. *International Permafrost Association*, 1–159.

Welch, H. E., & Legault, J. A. (1986). Precipitation Chemistry and Chemical Limnology of Fertilized and Natural Lakes at Saqvaqjuac, N.W.T. *Canadian Journal of Fisheries & Aquatic Sciences*, *43*.

Xiao, K., Griffis, T. J., Baker, J. M., Bolstad, P. V., Erickson, M. D., Lee, X., Wood, J. D., Hu, C., & Nieber, J. L. (2018). Evaporation from a temperate closed-basin lake and its impact on present, past, and future water level. *Journal of Hydrology*, *561*(March), 59–75. https://doi.org/10.1016/j.jhydrol.2018.03.059

Zaidi, F. K., Nazzal, Y., Jafri, M. K., Naeem, M., & Ahmed, I. (2015). Reverse ion exchange as a major process controlling the groundwater chemistry in an arid environment: a case study from northwestern Saudi Arabia. *Environmental Monitoring and Assessment*, *187*(10). https://doi.org/10.1007/s10661-015-4828-4

TABLES

Table 1: List of investigated water bodies and associated morphometric properties (lake type classification according to LeBlanc et al. (2022)).

Lake name	Latitude (°N)	Longitude (°E)	Surface area (m^2)	Maximum depth range (m)	Sampling year
Open talik basins					
DI3	62.921	-91.875	2.13E+07	NA	1995[a]
DI4	62.984	-92.051	8.25E+05	2 - 4	1995[a] & 2008[a]
Little Meliadine Lake	62.932	-92.259	7.36E+06	> 4	1998[a]; 2016[d]
Peter Lake	63.066	-92.811	1.80E+08	> 4	1998[a]
Lake Meliadine	63.111	-92.420	1.26E+08	> 4	1997-2000[a]; 2008-2009[a]; 2011[b]; 2015[c]; 2016[d]
Potential open talik basins					
A8	63.013	-92.205	8.87E+05	> 4	1994[a]; 1997-1998[a]; 2007-2009[a]; 2015[c]; 2016[d]
B2	63.007	-92.262	4.85E+05	2-4	1997-2000[a]; 2011[b]
B7	63.035	-92.252	5.67E+05	> 4	1997-1998[a]; 2008[a]; 2011[b]; 2015[c]
DI1 (Chicken Head Lake)	62.949	-91.920	1.35E+06	> 4	1994-1995[a]; 2008-2009[a]; 2015-2016[e]
Control Lake	63.009	-92.319	1.25E+06	> 4	1998-2000[a]; 2007-2009[a]; 2011[b]; 2016[d]
D7	63.028	-92.277	6.85E+05	2-4	1994[a]; 1997-1998[a]; 2011[b]; 2015[c]
DI5	62.977	-92.040	1.21E+06	NA	1995[a]
E3	63.047	-92.286	5.42E+05	> 4	1994[a]; 2011[b]; 2016[d]
Nipissar Lake	62.824	-92.126	1.11E+06	> 4	2016[d]
No open talik basins					
A1	62.999	-92.125	1.79E+05	2-4	1994[a] & 1997[a]
A13	63.025	-92.213	3.53E+03	< 2	2007[a] & 2016[d]
A15	63.026	-92.216	1.32E+03	NA	2007[a] & 2016[d]
A38	63.021	-92.200	4.90E+03	< 2	2007[a] & 2016[d]
A5	63.004	-92.155	1.83E+04	NA	1994[a]
A54	63.027	-92.206	5.84E+04	< 2	2007-2008[a]; 2016[d]
A56	63.028	-92.206	8.75E+02	NA	2007[a]
A57	63.027	-92.209	3.10E+03	NA	2007[a]
A6	63.001	-92.173	5.59E+05	> 4	1994[a]; 1998-2000[a]; 2004-2008[c]; 2009[a]; 2010-2016[e]
A9	63.021	-92.207	1.85E+04	< 2	2007[a] & 2016[d]
B36	63.009	-92.221	8.03E+04	< 2	1994[a]; 2011[b]
B45	62.999	-92.227	4.80E+05	2 - 4	2011[b]
B46	62.998	-92.206	4.48E+05	2 – 4	2011[b]
B5	63.024	-92.247	5.26E+05	2 – 4	1997-2000[a]; 2008[a]; 2011[b]; 2016[d]
B6	63.030	-92.253	1.10E+05	> 4	2008-2009[a]; 2011[b]
C5	62.991	-92.160	1.39E+05	NA	1994[a]
D23	63.034	-92.296	1.37E+05	2 – 4	2011[b]
D4	63.031	-92.312	1.74E+05	2 – 4	2011[b]
D5	63.032	-92.301	5.82E+04	2 – 4	2011[b]
DI2	62.971	-91.925	1.27E+05	NA	1994-1995[a]
E4	63.037	-92.273	7.61E+04	2 – 4	2011[b]
G2	63.044	-92.239	1.25E+05	2 – 4	1997[a]; 2004-2015[c]; 2016[d]
H1	63.034	-92.194	8.93E+03	< 2	2016[d]

Assessment of physicochemical properties in lentic water bodies of the Rankin Inlet area (Nunavut) for sublacustrine open talik detection.

H17	63.035	-92.211	1.57E+05	< 2	2011[b]; 2016[d]
H19	63.030	-92.197	2.77E+04	< 2	2016[d]
H20	63.027	-92.195	9.43E+04	< 2	2011[b]
Mel-Ctrl 6	63.102	-92.496	1.04E+04	NA	2004-2016[e]

[a]Golder (2012a)
[b]Golder (2012b)
[c]Golder (2016)
[d]Agnico Eagle Mines Ltd. (2016)
[e]CIRNAC-KIA (2020)

Table 2: Summary table of the Kruskal-Wallis rank-sum test. Bold values in the last column indicate significant (p-value < 0.05) intercategorical differences.

Variables	χ^2	df	p values
Specific conductivity (µS/cm^{-1})	13.04	2	**0.0015**
pH	16.6	2	**0.0002**
DO (%)	0.86	2	0.6514
TDS (ppm)	17.27	2	**0.0002**
Ca^{2+} (mEq/L)	19.06	2	**0.0001**
Cl^- (mEq/L)	5.58	2	0.0613
Mg^{2+} (mEq/L)	16.24	2	**0.0003**
Na^+ (mEq/L)	6.75	2	**0.0343**
SO_4^{2-} (mEq/L)	11.66	2	**0.0029**
HCO_3^- (mEq/L)	19.87	2	**0**
Ca/Cl (molar ratio)	1.35	2	0.509
Na/Cl (molar ratio)	5.4	2	0.0673
Mg/Cl (molar ratio)	0.36	2	0.8355
SO_4/Cl (molar ratio)	1.77	2	0.4125
HCO_3/Cl (molar ratio)	0.66	2	0.7201

Table 3: Summary table of the multiple comparison test after Kruskal-Wallis. Bold values in the last column indicate significant (p-value < 0.05) intercategorical differences.

Variables	Groups		Observed difference	Critical difference	p-value < 0.05
Specific conductivity (µS/cm^{-1})	POT	NOT	10.85	11.25	No
	OT	NOT	18.87	14.26	**Yes**
	POT	OT	8.02	16.38	No
pH	POT	NOT	14.61	10.38	**Yes**
	OT	NOT	21.32	14.05	**Yes**
	POT	OT	6.71	15.47	No
DO (%)	POT	NOT	0.00	7.20	No
	OT	NOT	2.71	7.89	No
	POT	OT	2.71	7.89	No
TDS (ppm)	POT	NOT	11.13	10.38	**Yes**
	OT	NOT	22.08	14.05	**Yes**
	POT	OT	10.95	15.47	No
Ca^{2+} (mEq/L)	POT	NOT	12.35	10.38	**Yes**
	OT	NOT	22.68	14.05	**Yes**
	POT	OT	10.33	15.47	No
Cl^- (mEq/L)	POT	NOT	7.40	10.38	No
	OT	NOT	11.60	14.05	No
	POT	OT	4.20	15.47	No
Mg^{2+} (mEq/L)	POT	NOT	11.33	10.38	**Yes**
	OT	NOT	21.00	14.05	**Yes**
	POT	OT	9.67	15.47	No

Na^+ (mEq/L)	POT	NOT	10.66	10.38	**Yes**
	OT	NOT	8.04	14.05	No
	POT	OT	2.62	15.47	No
SO_4^{2-} (mEq/L)	POT	NOT	11.77	10.38	**Yes**
	OT	NOT	15.44	14.05	**Yes**
	POT	OT	3.67	15.47	No
HCO_3^- (mEq/L)	POT	NOT	13.32	10.38	**Yes**
	OT	NOT	22.52	14.05	**Yes**
	POT	OT	9.20	15.47	No
Ca/Cl (molar)	POT	NOT	0.54	10.38	No
	OT	NOT	6.44	14.05	No
	POT	OT	6.98	15.47	No
Na/Cl (molar)	POT	NOT	5.72	10.38	No
	OT	NOT	12.68	14.05	No
	POT	OT	6.96	15.47	No
Mg/Cl (molar)	POT	NOT	0.21	10.38	No
	OT	NOT	3.48	14.05	No
	POT	OT	3.27	15.47	No
SO_4/Cl (molar)	POT	NOT	2.86	10.38	No
	OT	NOT	7.48	14.05	No
	POT	OT	4.62	15.47	No
HCO_3/Cl (molar)	POT	NOT	0.64	10.38	No
	OT	NOT	4.36	14.05	No
	POT	OT	5.00	15.47	No

Table 4: Mean values for physicochemical properties in lake groupings clustered according to an unsupervised machine learning hierarchical analysis.

	pH	**Specific conductivity ($\mu S/cm^{-1}$)**	**Ca^{2+} (mEq/L)**	**Cl^- (mEq/L)**	**Mg^{2+} (mEq/L)**	**Na^+ (mEq/L)**	**SO_4^{2-} (mEq/L)**	**HCO_3^- (mEq/L)**	**TDS (ppm)**
Cluster #1	7.98	1418	13.47	14.83	2.32	1.32	0.49	1.04	875.63
Cluster #2	7.66	140	0.81	0.45	0.19	0.20	0.05	0.67	82.26

Table 5: Predicted hydrochemical evolution of surficial waters in no open talik lakes under evaporation.

Evaporative model (pCO_2 = -3.00 atm.)

Concentration factor	pH	Ca^{2+} (molar)	Na^{+} (molar)	Mg^{2+} (molar)	Cl^{-} (molar)	SO_4^{2-} (molar)	HCO_3^{-} (molar)	Ca/Cl	Na/Cl	Mg/Cl	SO_4/Cl	HCO_3/Cl
1	7.39	1.55E-04	1.44E-04	3.86E-05	1.73E-04	1.45E-05	3.11E-04	8.98E-01	8.30E-01	2.23E-01	8.37E-02	1.80E+00
2	7.594	3.11E-04	2.87E-04	7.73E-05	3.46E-04	2.90E-05	6.19E-04	8.98E-01	8.30E-01	2.23E-01	8.37E-02	1.79E+00
4	7.882	6.21E-04	5.74E-04	1.55E-04	6.91E-04	5.79E-05	1.22E-03	8.98E-01	8.30E-01	2.23E-01	8.37E-02	1.77E+00
8	7.962	7.57E-04	1.15E-03	3.09E-04	1.38E-03	1.16E-04	1.49E-03	5.48E-01	8.30E-01	2.23E-01	8.37E-02	1.08E+00
16	7.97	7.76E-04	2.29E-03	6.17E-04	2.76E-03	2.31E-04	1.54E-03	2.81E-01	8.30E-01	2.23E-01	8.37E-02	5.56E-01
32	7.983	8.02E-04	4.58E-03	1.23E-03	5.51E-03	4.62E-04	1.61E-03	1.46E-01	8.30E-01	2.23E-01	8.37E-02	2.93E-01

Evaporative model (pCO_2 = -3.43 atm.)

Concentration factor	pH	Ca^{2+} (molar)	Na^{+} (molar)	Mg^{2+} (molar)	Cl^{-} (molar)	SO_4^{2-} (molar)	HCO_3^{-} (molar)	Ca/Cl	Na/Cl	Mg/Cl	SO_4/Cl	HCO_3/Cl
1	7.39	1.55E-04	1.43E-04	3.86E-05	1.73E-04	1.45E-05	3.11E-04	8.96E-01	8.27E-01	2.23E-01	8.38E-02	1.80E+00
2	8.02E+00	3.11E-04	2.87E-04	7.73E-05	3.46E-04	2.90E-05	6.13E-04	8.99E-01	8.29E-01	2.23E-01	8.38E-02	1.77E+00
4	8.24	5.33E-04	5.74E-04	1.55E-04	6.91E-04	5.79E-05	1.03E-03	7.71E-01	8.31E-01	2.24E-01	8.38E-02	1.49E+00
8	8.246	5.42E-04	1.15E-03	3.09E-04	1.38E-03	1.16E-04	1.06E-03	3.93E-01	8.33E-01	2.24E-01	8.41E-02	7.68E-01
16	8.255	5.56E-04	2.29E-03	6.17E-04	2.76E-03	2.31E-04	1.10E-03	2.01E-01	8.30E-01	2.24E-01	8.37E-02	3.99E-01
32	8.268	5.74E-04	4.58E-03	1.23E-03	5.51E-03	4.62E-04	1.15E-03	1.04E-01	8.31E-01	2.23E-01	8.38E-02	2.09E-01

FIGURES

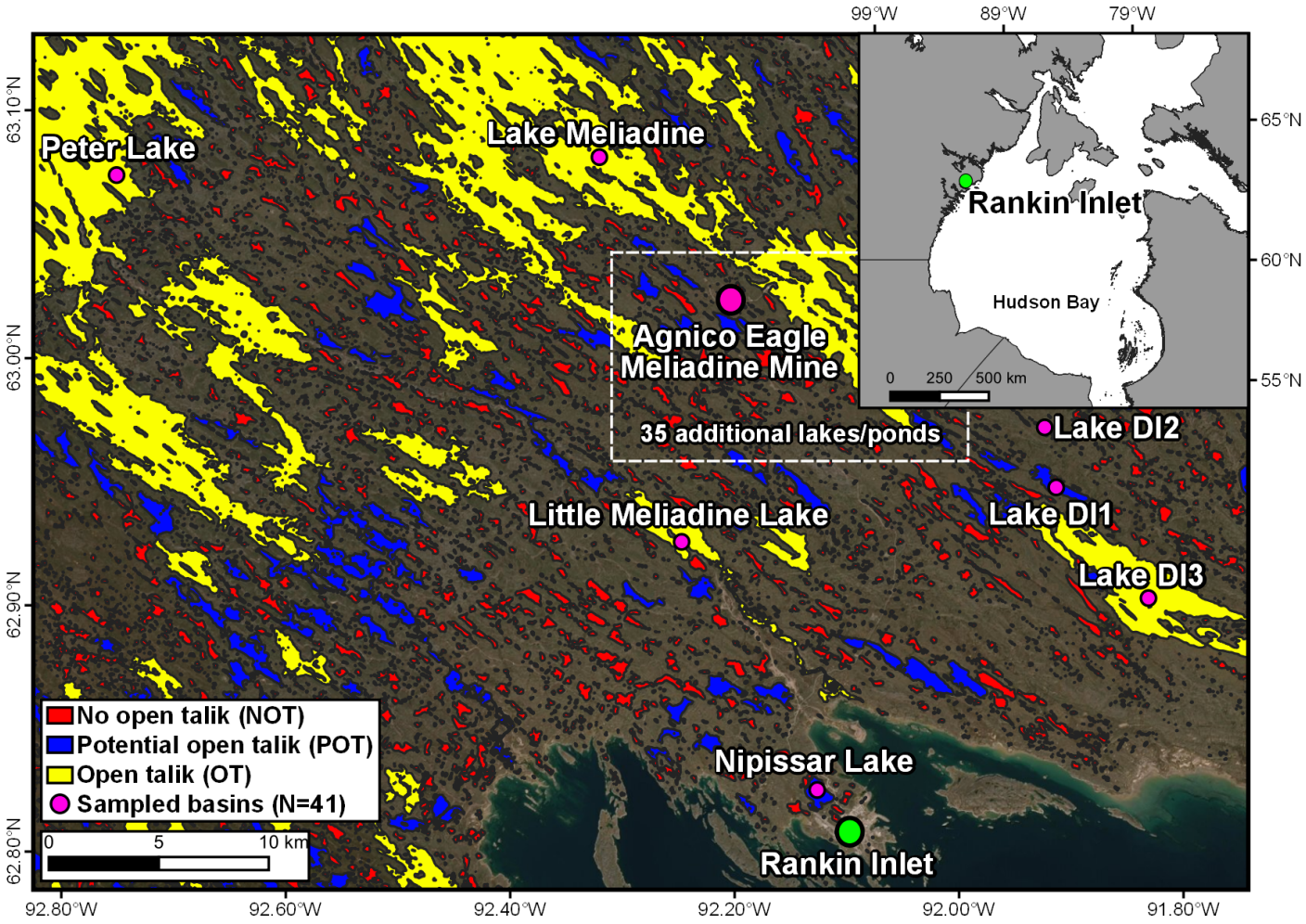

Figure 1: Location map of Rankin Inlet (Nunavut; green dot), the Agnico Eagle Meliadine Mine (large pink circle), and surface water bodies (small pink circles) investigated in this study. Lakes and ponds (N=41) are classified according to LeBlanc et al. (2022) as open (yellow; OT), potential (blue; POT), or no open (red; NOT) talik basins. The background is a 2.5m *SPOT* Imagery image of the area of interest acquired via QGIS' "Quick Map Services" plugin.

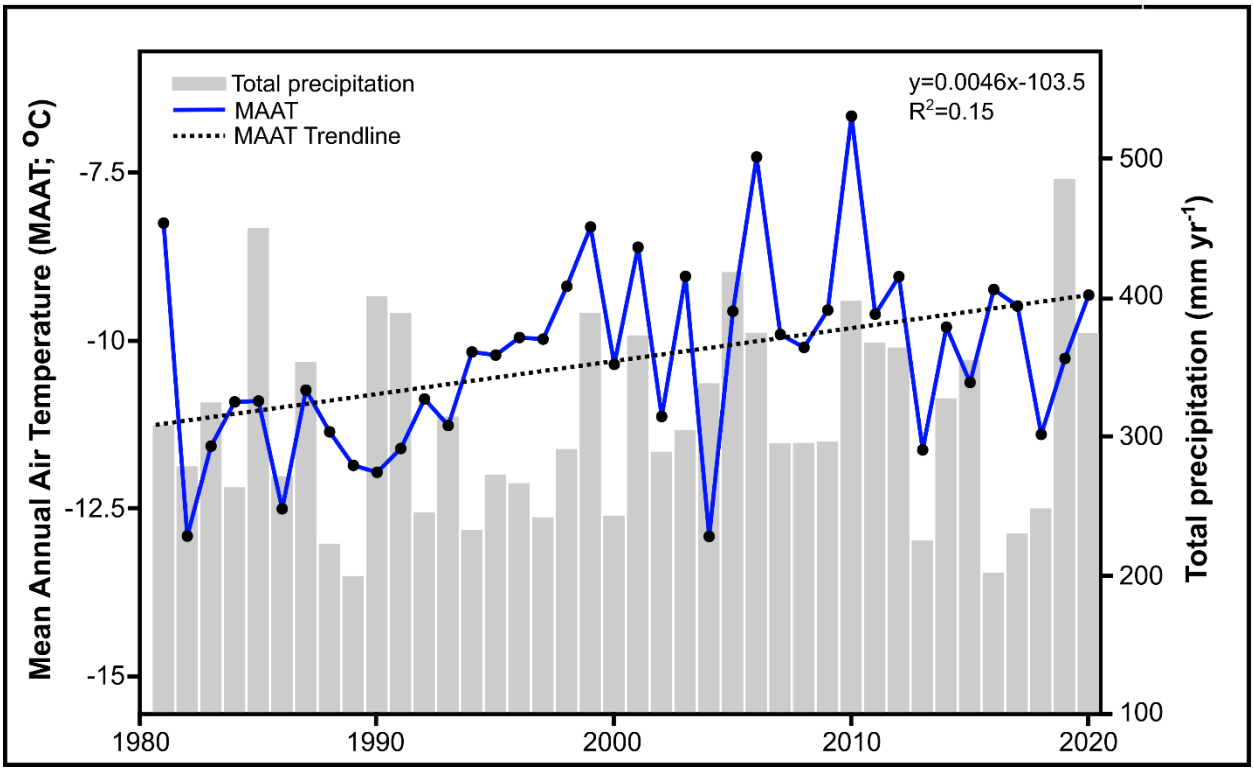

Figure 2: Time-series line and bar chart showing Rankin Inlet's Mean Annual Air Temperature (MAAT; °C) and total precipitation (mm yr^{-1}) during the 1981-2020 period. Data were taken from the Government of Canada's Historical Climate Data website (https://climate.weather.gc.ca/index_e.html).

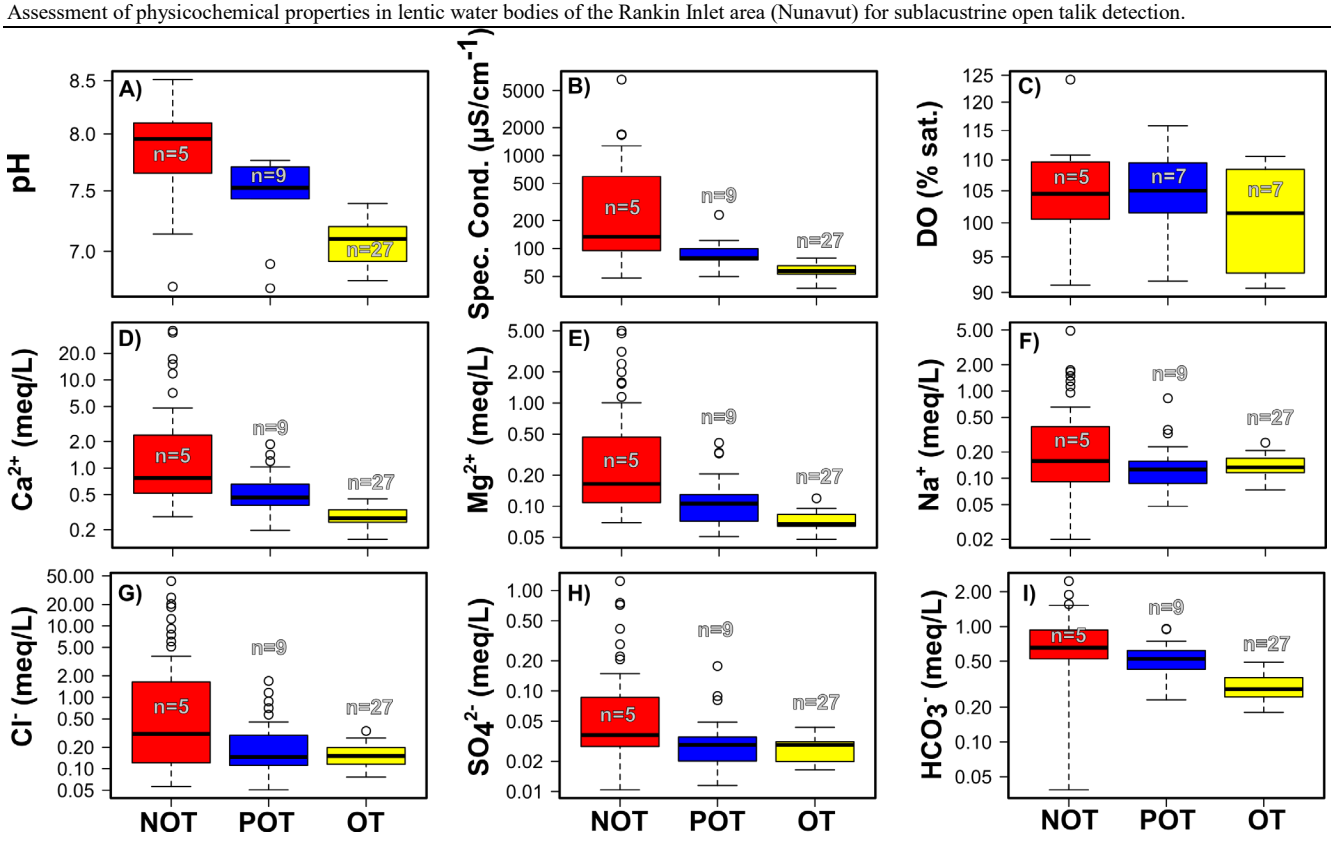

Figure 3: Physicochemical properties in open talik (OT), potential open talik (POT), and no open talik (NOT) lakes and ponds of the Rankin Inlet area. Number of lentic basins included in boxplots in shown in each panel.

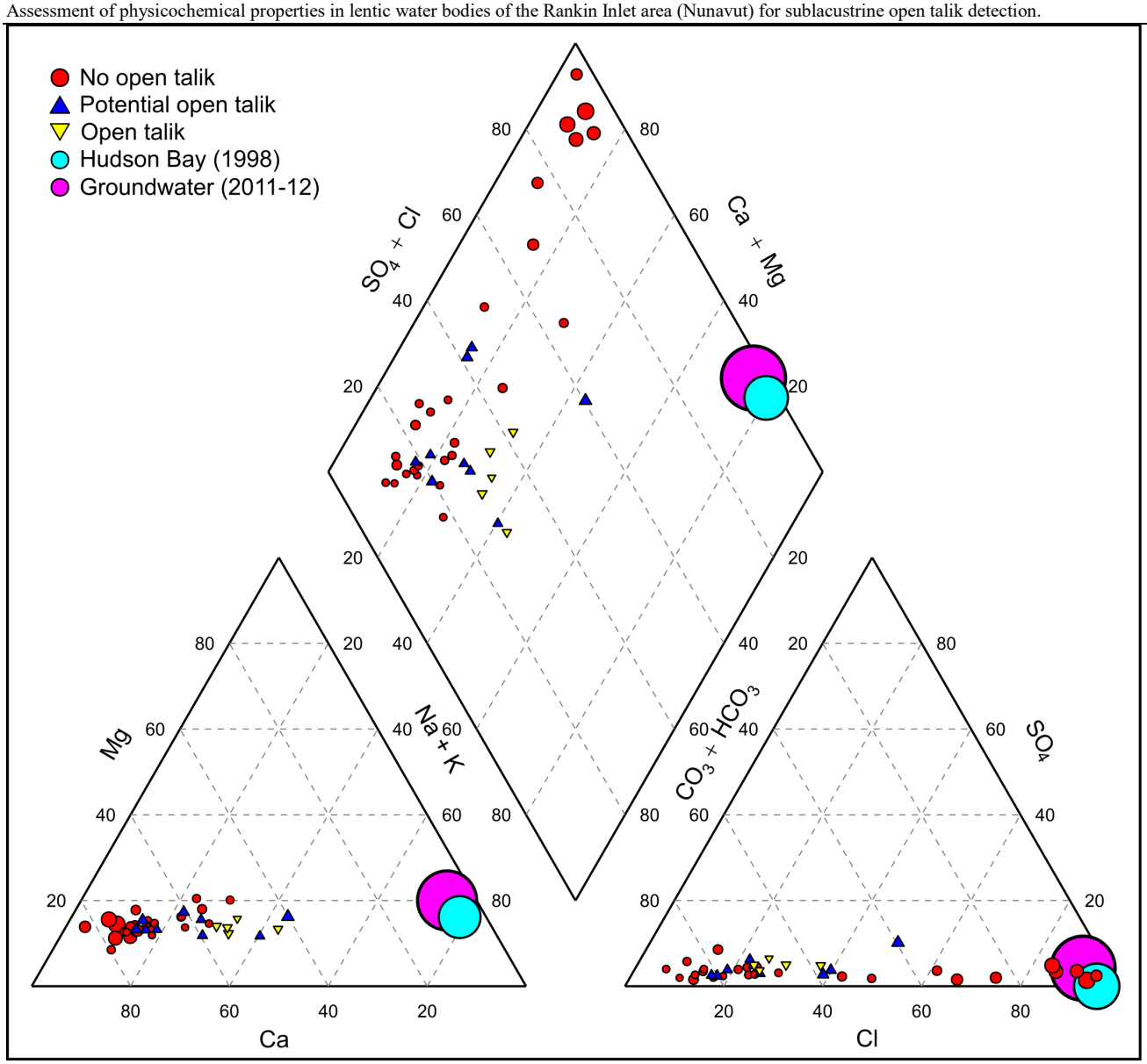

Figure 4: Piper diagram displaying the hydrochemical facies of sampled lakes and ponds in the Rankin Inlet area. Data for the Hudson Bay and subpermafrost groundwater added for comparison (Golder, 2016). Dot size is indicative of dissolved ionic load (i.e., bigger do size = higher solute load and vice-versa).

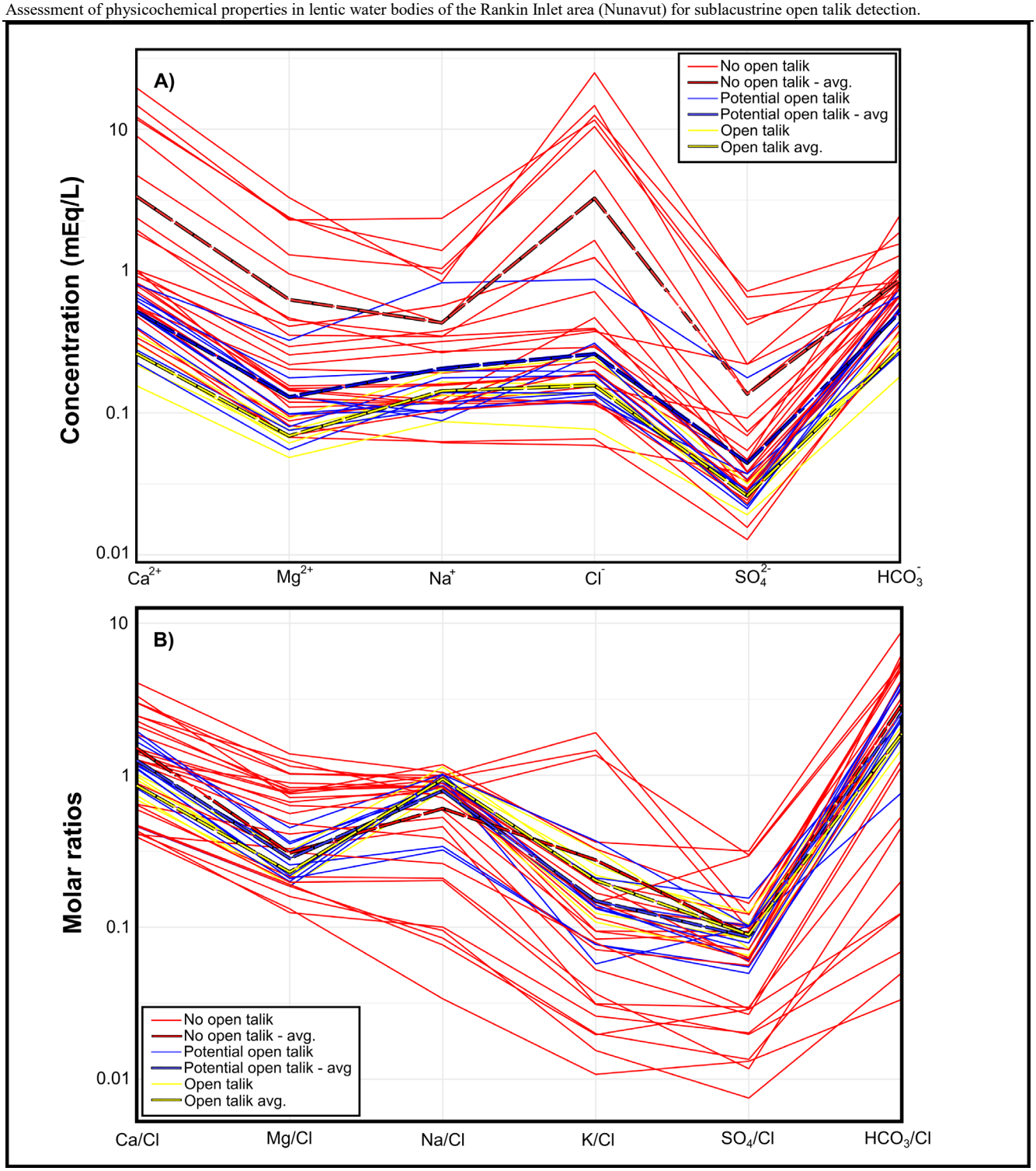

Figure 5: Schoeller diagrams for Rankin Inlet area lakes and ponds. A) Concentrations of major ions (mEq/L); and B) Cl^- normalized molar ratios for Ca^{2+}, Mg^{2+}, Na^+, K^+, SO_4^{2-}, and HCO_3^-.

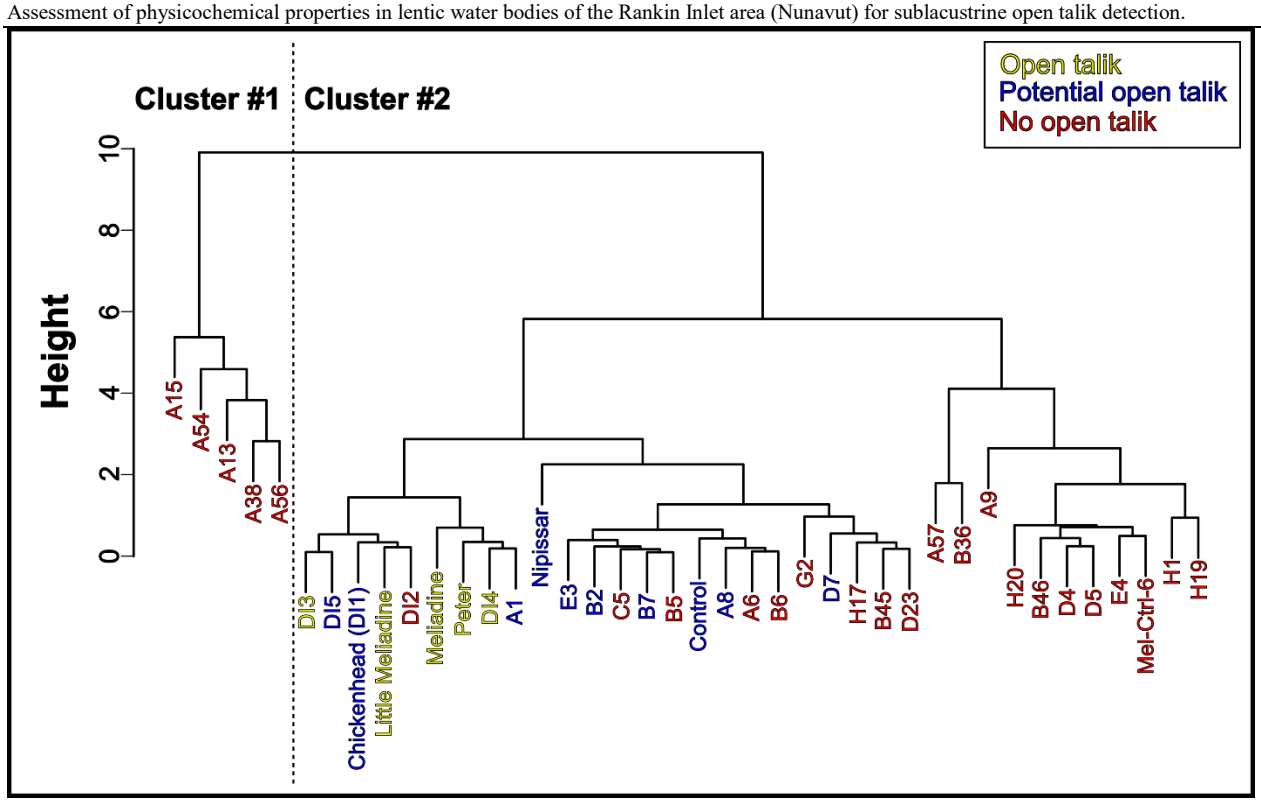

Figure 6: Hierarchical cluster of Rankin Inlet lentic basins according to their physicochemical properties. The first cluster is composed of five no open talik lakes. The second group (n=36) encompasses open, no open and potential open talik lakes seemingly sharing enough in common to be joined together.

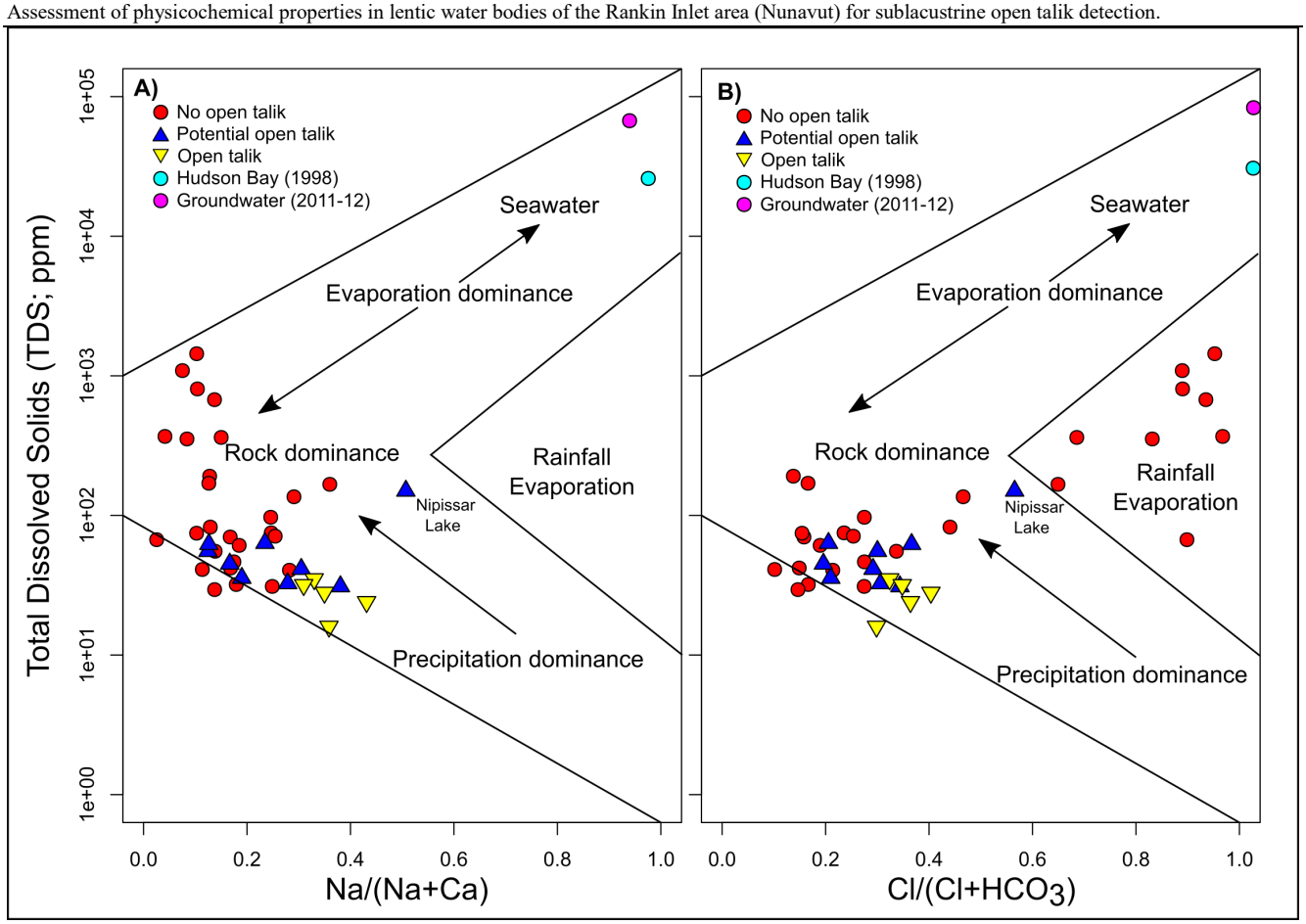

Figure 7: Gibbs diagram showing main processes controlling the hydrochemistry of lentic basins in the Rankin Inlet area. A) Comparison between TDS and Na/(Na+Ca). B) Comparison between TDS and Cl/(Cl+HCO_3). Data for the Hudson Bay and subpermafrost groundwater were added for comparison (Golder, 2016).

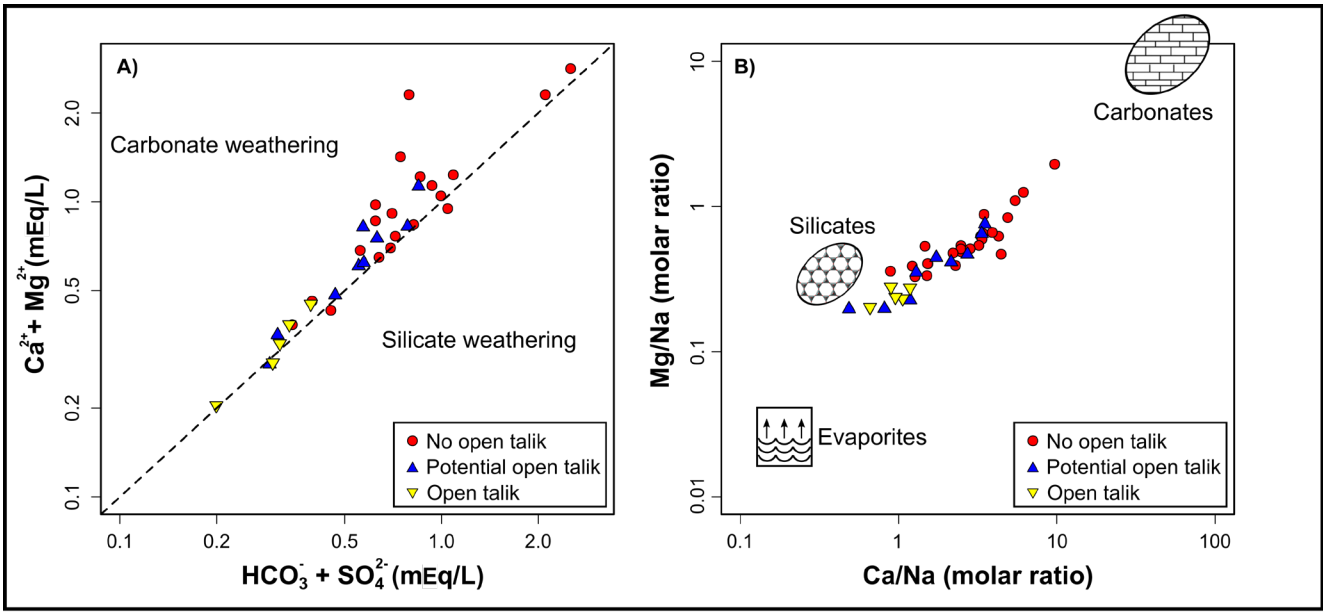

Figure 8: A) Scatter plot of Ca^{2+} + Mg^{2+} vs. HCO_3^- + SO_4^{2-}. B) Scatter plot of Mg^{2+}/Na^+ vs. Ca^{2+}/Na^+. End member values for evaporites, silicates and carbonates are taken from Gaillardet et al. (1999).

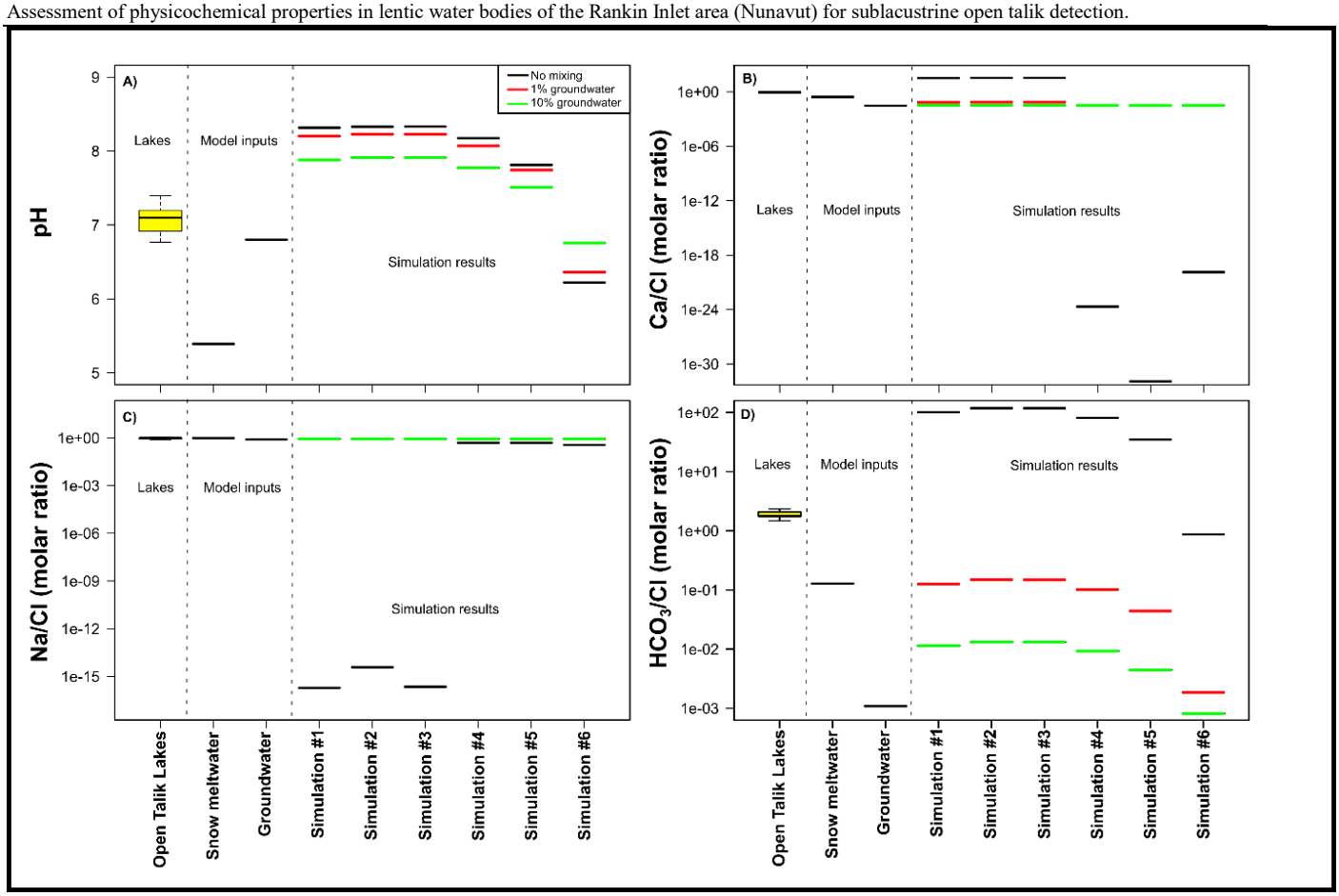

Figure 9: Boxplots showing chemical weathering simulation results. Predicted pH, Ca^{2+}/Cl^-, Na^+/Cl^-, and HCO_3^-/Cl^- values under six different weathering and two-component mixing scenarios are respectively shown in panels A to D. The model attempts to predict the chemical composition of nearby atmospherically equilibrated precipitation once it has fully reacted with various minerals assemblages. It then mixes the results from the weathering simulations with either 1 or 10% lentic basin water volume with groundwaters. Simulation #1=Greenstone & Granite rich tills + carbonates (calcite & dolomite); Simulation #2=Greenstone rich till + carbonates (calcite & dolomite); Simulation #3=Granite rich till + carbonates (calcite & dolomite); Simulation #4=Greenstone & Granite rich tills; Simulation #5=Greenstone rich till; Simulation #6=Granite rich till. The chemical composition of snow meltwaters and groundwaters were taken from Welch & Legault (1986) and Golder (2016), respectively.

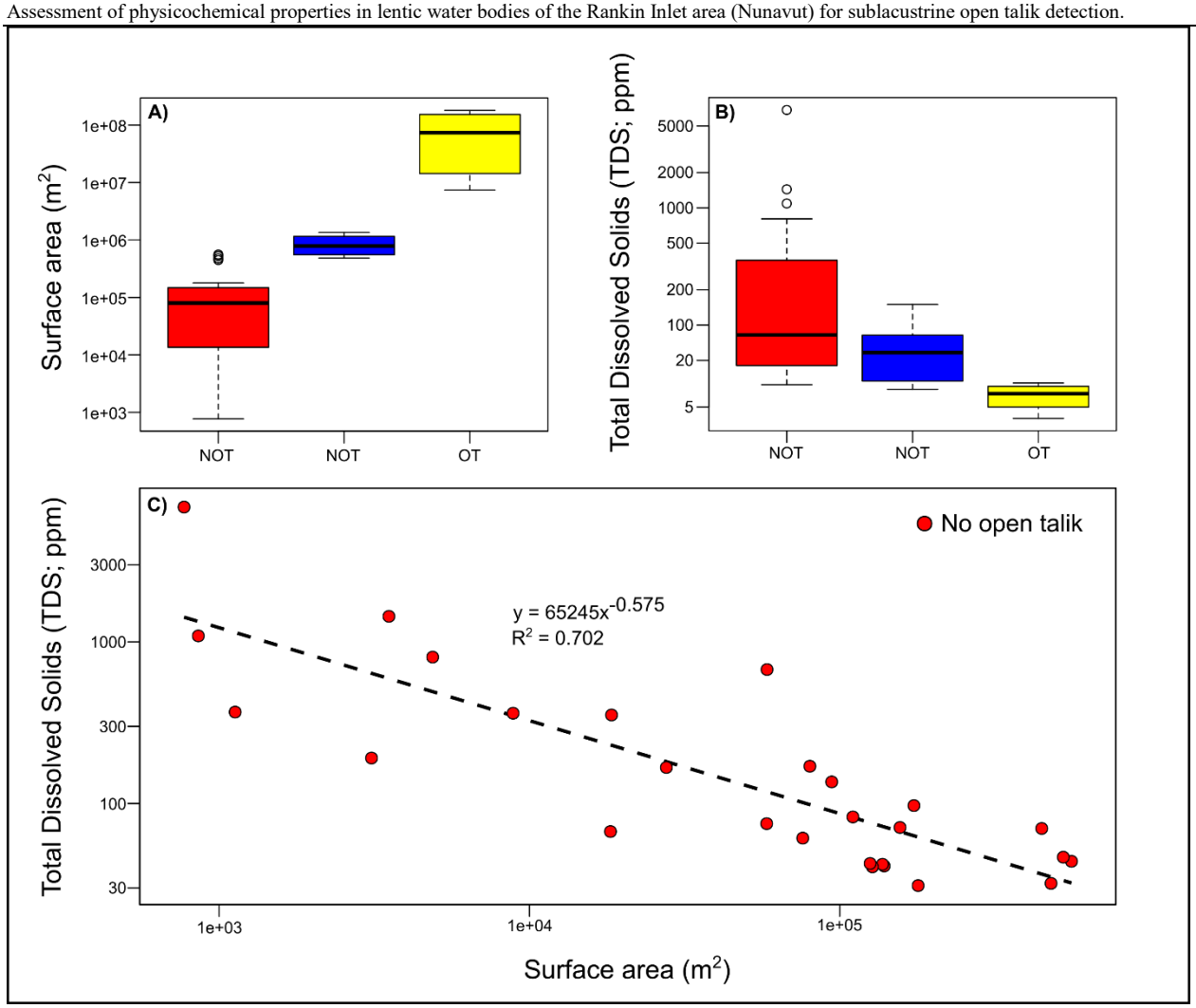

Figure 10: A) Boxplot showing the range of surface area (m^2) values within lake type; B) Boxplot showing the range of Total Dissolved Solids (TDS; ppm) within lakes types; and C) log-log scatterplot showing the negative correlation between TDS values and surface area for no open talik lakes.

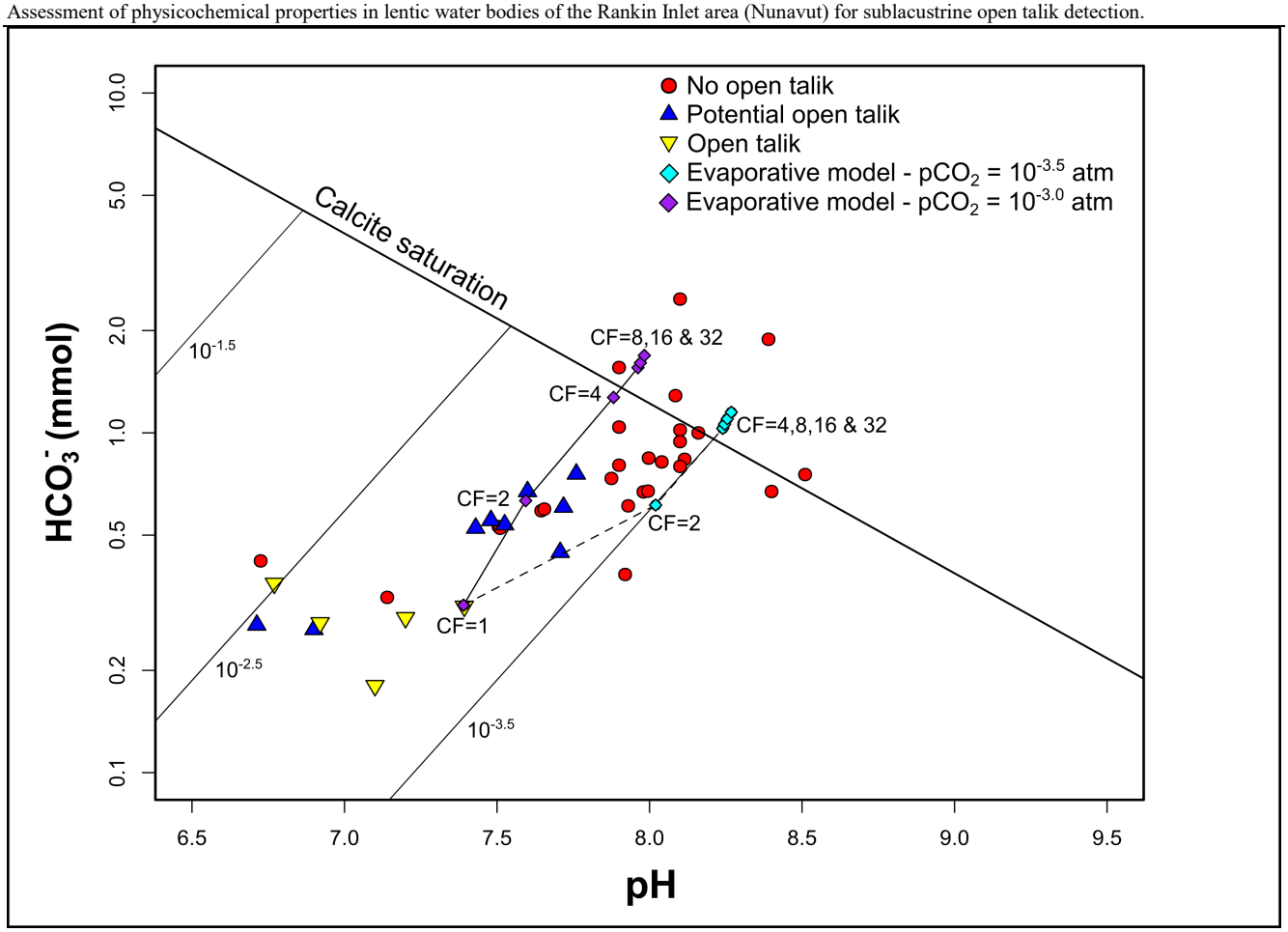

Figure 11: Predicted evolution of bicarbonate (HCO_3^-) and pH in no open talik lakes, under evaporation modelling. CF=concentration factor.

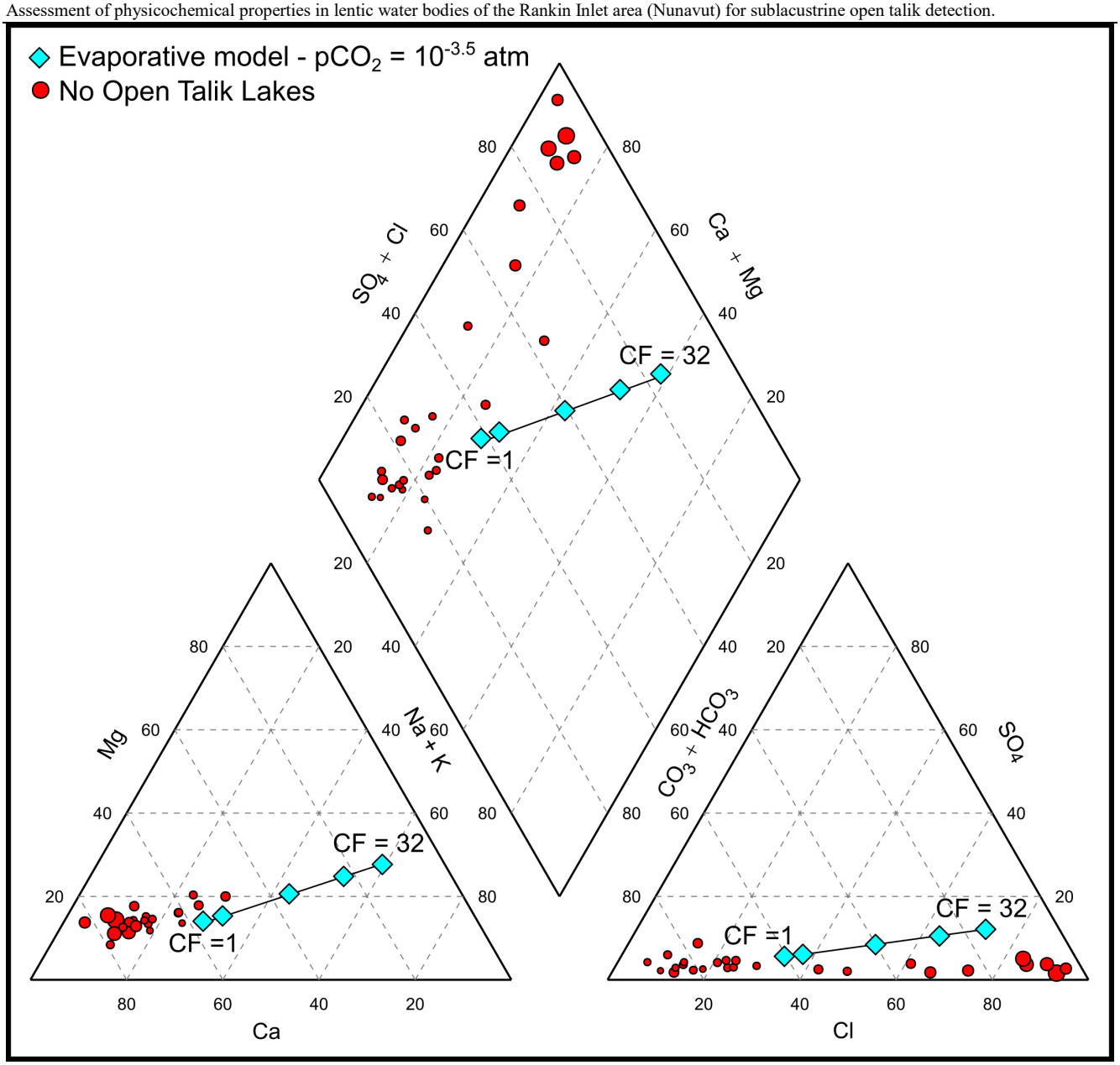

Figure 12: Piper diagram showing the predicted hydrochemical evolution of no open talik water bodies affected by evaporation. Dot size is indicative of dissolved ionic load (i.e., bigger do size = higher solute load and vice-versa).

APPENDIX

Table A1: Molar concentrations and ratios for greenstone- and/or granite-rich till weathering simulations.

	pH	Ca^{2+} (molar)	Na^{+} (molar)	Mg^{2+} (molar)	Cl^{-} (molar)	HCO_3^{-} (molar)	Ca/Cl (molar)	Na/Cl (molar)	HCO_3/Cl (molar)
Saqvaqjuac snow	5.6	3.39E-06	1.17E-05	1.56E-06	1.24E-05	NA	2.73E-01	9.46E-01	NA
Saqvaqjuac snow (atm CO_2 equilibrated; $_PCO_2$ = -3.43)	5.39	3.39E-06	1.17E-05	1.56E-06	1.24E-05	1.59E-06	2.73E-01	9.46E-01	1.28E-01
Groundwater	6.8	2.69E-02	7.39E-01	9.22E-02	9.17E-01	1.00E-03	2.93E-02	8.05E-01	1.09E-03
Open talik lakes									
Lake DI3	6.92	1.09E-04	1.65E-04	3.34E-05	1.58E-04	2.76E-04	6.90E-01	1.05E+00	1.75E+00
Lake DI4	7.2	1.35E-04	1.33E-04	3.07E-05	1.37E-04	2.86E-04	9.85E-01	9.70E-01	2.09E+00
Little Meliadine Lake	6.77	1.80E-04	1.93E-04	4.59E-05	2.44E-04	3.61E-04	7.36E-01	7.92E-01	1.48E+00
Lake Meliadine	7.3928	1.55E-04	1.43E-04	3.86E-05	1.73E-04	3.13E-04	8.98E-01	8.30E-01	1.81E+00
Peter Lake	7.1	7.78E-05	8.70E-05	2.43E-05	7.67E-05	1.80E-04	1.01E+00	1.13E+00	2.35E+00
Simulation #1: Greenstone & Granite riche tills with carbonates	8.316	4.60E-04	2.63E-21	2.83E-04	1.39E-05	1.41E-03	3.30E+01	1.89E-16	1.01E+02
0.01% Groundwater mixing	8.314	4.63E-04	9.25E-05	2.94E-04	1.23E-04	1.41E-03	3.77E+00	7.55E-01	1.15E+01
0.1% Groundwater mixing	8.299	4.91E-04	9.25E-04	3.86E-04	1.10E-03	1.40E-03	4.46E-01	8.41E-01	1.27E+00
1% Groundwater mixing	8.202	7.73E-04	9.24E-03	1.31E-03	1.09E-02	1.38E-03	7.12E-02	8.51E-01	1.27E-01
10% Groundwater mixing	7.881	3.56E-03	9.14E-02	1.05E-02	1.07E-01	1.22E-03	3.32E-02	8.51E-01	1.14E-02
Simulation #2: Greenstone rich till with carbonates	8.33	4.26E-04	4.60E-20	3.43E-04	1.24E-05	1.47E-03	3.43E+01	3.71E-15	1.18E+02
0.01% Groundwater mixing	8.332	4.29E-04	8.25E-05	3.52E-04	1.09E-04	1.47E-03	3.92E+00	7.55E-01	1.34E+01
0.1% Groundwater mixing	8.318	4.54E-04	8.25E-04	4.34E-04	9.81E-04	1.46E-03	4.63E-01	8.41E-01	1.49E+00
1% Groundwater mixing	8.226	7.07E-04	8.25E-03	1.26E-03	9.70E-03	1.44E-03	7.28E-02	8.51E-01	1.48E-01
10% Groundwater mixing	7.913	3.23E-03	8.25E-02	9.52E-03	9.69E-02	1.28E-03	3.33E-02	8.52E-01	1.32E-02
Simulation #3: Granite rich till with carbonates	8.333	4.28E-04	2.76E-21	3.44E-04	1.24E-05	1.46E-03	3.45E+01	2.22E-16	1.18E+02
0.01% Groundwater mixing	8.331	4.30E-04	8.25E-05	3.53E-04	1.09E-04	1.46E-03	3.94E+00	7.55E-01	1.34E+01
0.1% Groundwater mixing	8.318	4.56E-04	8.25E-04	4.36E-04	9.81E-04	1.46E-03	4.64E-01	8.41E-01	1.49E+00
1% Groundwater mixing	8.227	7.08E-04	8.25E-03	1.26E-03	9.70E-03	1.44E-03	7.30E-02	8.51E-01	1.48E-01
10% Groundwater mixing	7.917	3.23E-03	8.25E-02	9.52E-03	9.69E-02	1.28E-03	3.34E-02	8.52E-01	1.32E-02
Simulation #4: Greenstone & Granite rich tills	8.174	2.61E-29	6.06E-06	5.25E-04	1.24E-05	1.01E-03	2.10E-24	4.88E-01	8.11E+01
0.01% Groundwater mixing	8.173	2.85E-06	8.86E-05	5.34E-04	1.09E-04	1.01E-03	2.61E-02	8.11E-01	9.21E+00
0.1% Groundwater mixing	8.158	2.85E-05	8.31E-04	6.16E-04	9.81E-04	1.01E-03	2.90E-02	8.47E-01	1.02E+00
1% Groundwater mixing	8.07	2.85E-04	8.26E-03	1.44E-03	9.70E-03	9.90E-04	2.94E-02	8.51E-01	1.02E-01
10% Groundwater mixing	7.772	2.85E-03	8.25E-02	9.68E-03	9.69E-02	9.03E-04	2.94E-02	8.52E-01	9.32E-03
Simulation #5: Greenstone rich till	7.813	1.49E-37	6.06E-06	2.76E-04	1.24E-05	4.33E-04	1.20E-32	4.88E-01	3.49E+01
0.01% Groundwater mixing	7.812	2.85E-06	8.86E-05	2.85E-04	1.09E-04	4.33E-04	2.61E-02	8.11E-01	3.96E+00
0.1% Groundwater mixing	7.801	2.85E-05	8.31E-04	3.67E-04	9.81E-04	4.33E-04	2.90E-02	8.47E-01	4.41E-01
1% Groundwater mixing	7.743	2.85E-04	8.26E-03	1.19E-03	9.70E-03	4.31E-04	2.94E-02	8.51E-01	4.44E-02
10% Groundwater mixing	7.513	2.85E-03	8.25E-02	9.46E-03	9.69E-02	4.31E-04	2.94E-02	8.52E-01	4.44E-03

Simulation #6: Granite rich till	6.221	1.67E-25	4.48E-06	1.52E-06	1.24E-05	1.08E-05	1.35E-20	3.61E-01	8.71E-01
0.01% Groundwater mixing	6.221	2.85E-06	8.70E-05	1.07E-05	1.09E-04	1.09E-05	2.61E-02	7.96E-01	9.97E-02
0.1% Groundwater mixing	6.234	2.85E-05	8.30E-04	9.36E-05	9.81E-04	1.16E-05	2.90E-02	8.46E-01	1.18E-02
1% Groundwater mixing	6.363	2.85E-04	8.26E-03	9.22E-04	9.70E-03	1.79E-05	2.94E-02	8.51E-01	1.84E-03
10% Groundwater mixing	6.759	2.85E-03	8.25E-02	9.21E-03	9.69E-02	7.94E-05	2.94E-02	8.52E-01	8.19E-04

Table A2: Saturation Indices (SI) for anhydrite, aragonite, calcite, dolomite, gypsum, halite and sylvite for lentic water basins situated within the Rankin Inlet area. OT = Open Talik basins; POT = Potential Open Talik basins; NOT = No Open Talik basins.

Lake Class	Lake ID	SI Anhydrite	SI Aragonite	SI Calcite	SI Dolomite	SI Gypsum	SI Halite	SI Sylvite
OT	DI3	-4.84	-2.82	-2.67	-5.77	-4.42	-9.17	-8.97
OT	DI4	-4.66	-2.42	-2.28	-5.12	-4.24	-9.33	-9.19
OT	LML	-4.50	-2.58	-2.44	-5.38	-4.09	-8.92	-9.07
OT	MEL	-4.59	-2.15	-2.01	-4.52	-4.18	-9.19	-9.33
OT	Peter Lake	-5.04	-2.95	-2.81	-6.04	-4.62	-9.76	-9.76
POT	A8	-4.39	-1.25	-1.11	-2.79	-3.97	-9.24	-9.17
POT	B2	-4.41	-1.67	-1.53	-3.68	-4.00	-9.37	-9.43
POT	B7	-4.22	-1.44	-1.30	-3.23	-3.80	-9.11	-9.01
POT	Chickenhead (DI1)	-4.53	-2.88	-2.74	-5.96	-4.11	-9.48	-9.39
POT	Control	-4.61	-1.56	-1.42	-3.44	-4.19	-9.08	-9.20
POT	D7	-4.34	-1.08	-0.94	-2.35	-3.93	-9.01	-9.18
POT	DI5	-4.73	-2.84	-2.70	-5.91	-4.31	-9.30	-9.02
POT	E3	-4.53	-1.58	-1.43	-3.50	-4.11	-9.44	-9.50
POT	Nipissar	-3.50	-1.24	-1.10	-2.50	-3.08	-7.75	-8.26
NOT	A1	-4.88	-2.38	-2.23	-5.03	-4.46	-8.58	-9.53
NOT	A13	-2.64	0.11	0.25	-0.12	-2.22	-6.38	-6.46
NOT	A15	-2.08	0.66	0.81	0.94	-1.67	-6.39	-6.18
NOT	A38	-2.41	0.28	0.42	0.1	-1.99	-6.64	-6.51
NOT	A5	-3.78	-1.37	-1.23	-3.09	-3.36	NA	-9.05
NOT	A54	-2.27	0.06	0.21	-0.30	-1.85	-6.26	-6.36
NOT	A56	-2.14	0.58	0.72	0.84	-1.72	-6.61	-6.49
NOT	A57	-3.67	-0.37	-0.22	-1.08	-3.25	-8.48	-7.92
NOT	A6	-4.23	-1.04	-0.90	-2.41	-3.81	-9.06	-9.08
NOT	A9	-3.03	-0.23	-0.08	-0.77	-2.61	-7.87	-7.21
NOT	B36	-3.08	-0.15	-0.01	-0.52	-2.67	-8.67	-8.59
NOT	B45	-4.38	-0.88	-0.73	-2.14	-3.97	-9.43	-8.43
NOT	B46	-4.04	-0.75	-0.60	-1.82	-3.63	-9.12	-9.04
NOT	B5	-4.38	-1.52	-1.38	-3.30	-3.96	-9.22	-9.30
NOT	B6	-4.28	-0.74	-0.59	-1.85	-3.87	-8.84	-8.65
NOT	C5	-4.32	-1.36	-1.22	-3.11	-3.91	-10.03	-9.78
NOT	D23	-4.43	-1.00	-0.86	-2.30	-4.02	-9.46	-9.61
NOT	D4	-3.81	-0.50	-0.36	-1.21	-3.39	-8.51	-8.80
NOT	D5	-3.96	-0.71	-0.57	-1.62	-3.55	-8.70	-8.99
NOT	DI2	-4.51	-2.52	-2.38	-5.26	-4.09	-9.41	-9.25
NOT	E4	-4.40	-0.67	-0.53	-1.62	-3.99	-9.14	-9.28
NOT	G2	-4.86	-1.14	-1.00	-2.67	-4.45	-9.98	-9.08
NOT	H1	-3.83	0.04	0.18	-0.29	-3.41	-7.86	-7.91
NOT	H17	-4.19	-0.98	-0.83	-2.01	-3.77	-8.96	-8.94
NOT	H19	-3.79	-0.26	-0.12	-0.55	-3.37	-7.76	-8.21
NOT	H20	-4.09	-0.65	-0.51	-1.42	-3.68	-8.17	-8.46
NOT	H3	NA	NA	NA	NA	NA	NA	NA
NOT	Mel Ctrl 6	-3.65	-0.61	-0.47	-1.82	-3.23	-9.35	-8.38